RSC Medicinal Chemistry

ROYAL SOCIETY OF CHEMISTRY

RESEARCH ARTICLE

View Article Online
View Journal | View Issue

Cite this: *RSC Med. Chem.*, 2020, **11**, 707

2-Arylamino-6-ethynylpurines are cysteine-targeting irreversible inhibitors of Nek2 kinase†

Christopher J. Matheson,‡[a] Christopher R. Coxon, ‡[a] Richard Bayliss, [cd] Kathy Boxall,‡[b] Benoit Carbain,[a] Andrew M. Fry, [c] Ian R. Hardcastle,[a] Suzannah J. Harnor, [a] Corine Mas-Droux,[d] David R. Newell,[e] Mark W. Richards,[c] Mangaleswaran Sivaprakasam,[a] David Turner,[a] Roger J. Griffin,§[a] Bernard T. Golding [a] and Céline Cano *[a]

Renewed interest in covalent inhibitors of enzymes implicated in disease states has afforded several agents targeted at protein kinases of relevance to cancers. We now report the design, synthesis and biological evaluation of 6-ethynylpurines that act as covalent inhibitors of Nek2 by capturing a cysteine residue (Cys22) close to the catalytic domain of this protein kinase. Examination of the crystal structure of the non-covalent inhibitor 3-((6-cyclohexylmethoxy-7*H*-purin-2-yl)amino)benzamide in complex with Nek2 indicated that replacing the alkoxy with an ethynyl group places the terminus of the alkyne close to Cys22 and in a position compatible with the stereoelectronic requirements of a Michael addition. A series of 6-ethynylpurines was prepared and a structure activity relationship (SAR) established for inhibition of Nek2. 6-Ethynyl-*N*-phenyl-7*H*-purin-2-amine [IC_{50} 0.15 μM (Nek2)] and 4-((6-ethynyl-7*H*-purin-2-yl)amino)benzenesulfonamide (IC_{50} 0.14 μM) were selected for determination of the mode of inhibition of Nek2, which was shown to be time-dependent, not reversed by addition of ATP and negated by site directed mutagenesis of Cys22 to alanine. Replacement of the ethynyl group by ethyl or cyano abrogated activity. Variation of substituents on the *N*-phenyl moiety for 6-ethynylpurines gave further SAR data for Nek2 inhibition. The data showed little correlation of activity with the nature of the substituent, indicating that after sufficient initial competitive binding to Nek2 subsequent covalent modification of Cys22 occurs in all cases. A typical activity profile was that for 2-(3-((6-ethynyl-9*H*-purin-2-yl)amino)phenyl)acetamide [IC_{50} 0.06 μM (Nek2); GI_{50} (SKBR3) 2.2 μM] which exhibited >5–10-fold selectivity for Nek2 over other kinases; it also showed > 50% growth inhibition at 10 μM concentration against selected breast and leukaemia cell lines. X-ray crystallographic analysis confirmed that binding of the compound to the Nek2 ATP-binding site resulted in covalent modification of Cys22. Further studies confirmed that 2-(3-((6-ethynyl-9*H*-purin-2-yl)amino)phenyl)acetamide has the attributes of a drug-like compound with good aqueous solubility, no inhibition of hERG at 25 μM and a good stability profile in human liver microsomes. It is concluded that 6-ethynylpurines are promising agents for cancer treatment by virtue of their selective inhibition of Nek2.

Received 4th March 2020,
Accepted 2nd May 2020

DOI: 10.1039/d0md00074d

rsc.li/medchem

[a] *Cancer Research UK Newcastle Drug Discovery Unit, Chemistry, School of Natural and Environmental Sciences, Newcastle University, Newcastle upon Tyne, UK. E-mail: celine.cano@ncl.ac.uk; Tel: +44 (0)191 208 7060*
[b] *Cancer Research UK Cancer Therapeutics Unit, The Institute of Cancer Research, Sutton, UK*
[c] *School of Molecular and Cellular Biology, The Astbury Centre for Structural Molecular Biology, University of Leeds, UK*
[d] *Section of Structural Biology, The Institute of Cancer Research, Sutton, UK*
[e] *Cancer Research UK Newcastle Drug Discovery Unit, Translational and Clinical Research Institute, Newcastle University Centre for Cancer, Faculty of Medical Sciences, Newcastle University, Newcastle upon Tyne, UK*

† Electronic supplementary information (ESI) available: Kinase profiling, assay details, synthetic procedures and characterisation data for all compounds; including aniline precursors. All cell lines were supplied by the American Type Culture Collection, Manassas, Virginia, United States. All animal experiments performed were conducted under a UK Government Home Office License in accordance with relevant national laws. All procedures were reviewed and approved by the Newcastle University Animal Welfare Ethical Board and performed according to institutional guidelines. See DOI: 10.1039/d0md00074d

‡ These authors contributed equally to the work described in this paper.

§ Deceased 24 September 2014.

Introduction

The renaissance in the development of inhibitors that bind covalently to a target enzyme either irreversibly or slowly reversibly has yielded several licensed agents, especially in the oncology area. As of 2019, six irreversible protein kinase inhibitors have received FDA approval for use in oncology (afatinib **1**, osimertinib, neratinib **2** and ibrutinib, dacomitinib and acalabrutinib, Fig. 1A). Afatanib (**1**), licensed in 2013 for treatment of metastatic NSCLC through irreversible inhibition of EGFR, and neratinib (**2**), approved in 2017 for treatment of HER2+ breast cancer, were designed as modifications of gefitinib (**3**) by installation of electrophilic acrylamide groups that target an active site cysteine. Protein kinases are prominent targets for covalent inhibitors, which owing to the high concentrations of ATP in cells (~1–10 mM)

may be more effective than competitive inhibitors because of irreversible ATP-blockade.[1] A range of warhead groups has been employed in irreversible protein kinase inhibitors, for example, acrylamides, alkynes, quinones and epoxides.[2] Previously, our group discovered the vinyl sulfone (NU6300) as the first irreversible inhibitor of CDK2 that was shown to react covalently with an active site lysine residue (Lys89) in the selectivity pocket.[3]

Nek2 is the closest human homologue of the protein kinase encoded by NIMA (never-in-mitosis gene A) in the fungus *Aspergillus nidulans*. The human protein is a serine–threonine kinase with multiple functions including a role in the mitotic spindle assembly. Overexpression of Nek2 may result in deregulation of the mitotic machinery leading to chromatid segregation errors, aneuploidy and chromosomal instability, common genetic abnormalities observed in tumour cells. Nek2 has been associated with tumorigenesis through overexpression, which has been linked to Ewing's osteosarcoma, diffuse large B-cell lymphoma, breast, ovarian and colorectal tumours.[4–9]

Inhibition of Nek2 in a number of tumour cell lines causes growth suppression and apoptosis. Reversible ATP-competitive Nek2 kinase inhibitors have been reported based on different structural classes, including: aminopyrazines (*e.g.*, **4** IC_{50} = 0.23 μM),[10] but with poor Nek2-selectivity over Plk1; benzimidazoles that exhibited >100-fold selectivity for Nek2 over Plk1 (*e.g.*, **5** IC_{50} = 0.36 μM), yet had poor cellular activity,[11] and a hybrid combining a core aminopyrazine moiety with side-chains from the benzimidazole series **6** (IC_{50} = 0.022 μM)[12] (Fig. 1B), which was potent and Nek2-selective. As Nek2 contains a non-catalytic cysteine (Cys22) close to the catalytic domain that is unique to the Nek family, this residue can be targeted for irreversible binding. Only 10 other kinases have a cysteine in a similar position.[13] One irreversible Nek2 inhibitor has been published (JH295, **7** IC_{50} = 0.77 μM),[13] which targeted Cys22 *via* an *N*-arylpropiolamide Michael acceptor and was reported to be selective against other mitotic kinases, including CDK1, PLK1, Aurora B and Mps1. Herein, we describe the design and synthesis of a new class of selective tool compounds that covalently and irreversibly inhibit the Nek2 protein kinase. Our studies provide an insight into the role of Nek2 in cancer and address the question as to whether Nek2 is truly an attractive target for anti-cancer drug design.

Results and discussion

To improve understanding of the role of Nek2 in cancer, we sought a selective inhibitor of Nek2 by targeting the active site Cys22 residue. We have discovered covalent inhibitors superior to compound 7, which was non-selective within a subset of the kinome investigated here (see ESI†) and was

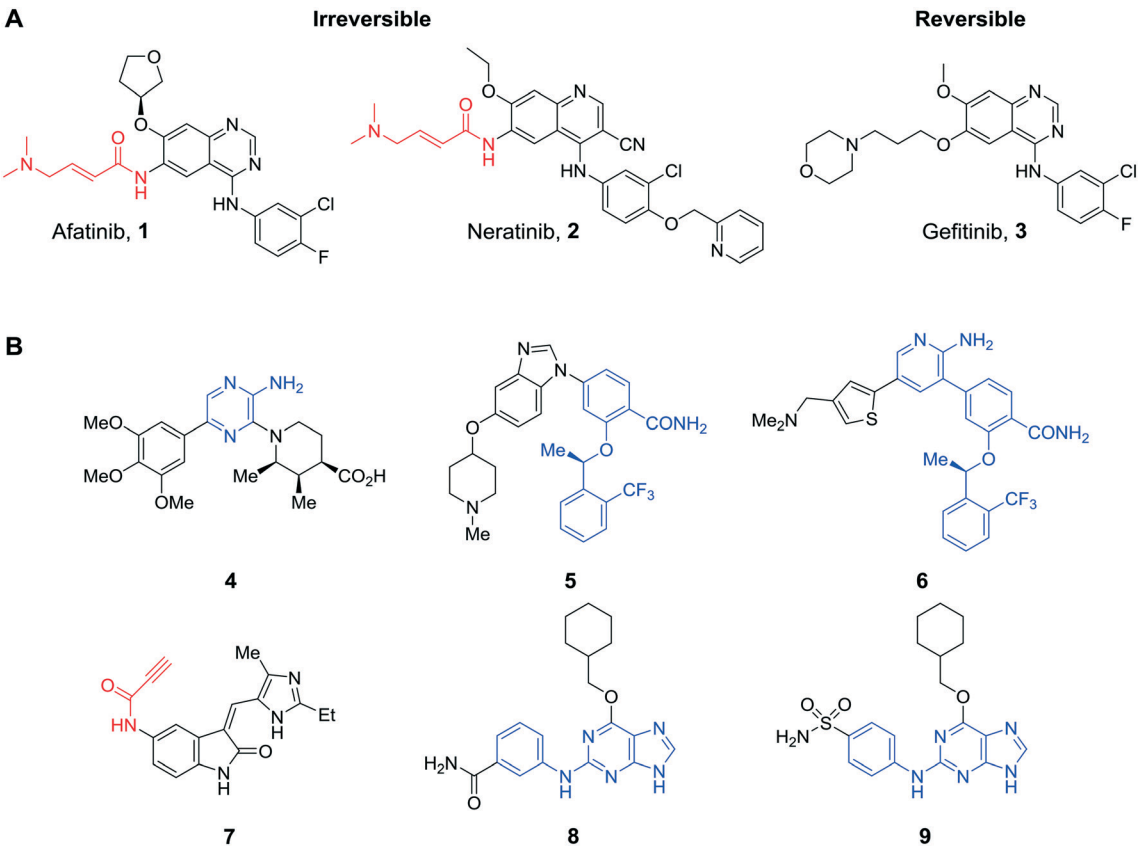

Fig. 1 A) Rationalisation of the modification of gefitinib (reversible) to afford afatinib and neratinib (irreversible). B) Reversible and irreversible reported inhibitors of Nek2 kinase. For each case, covalent 'warhead' groups are shown in red and core scaffolds in blue.

therefore inadequate for further studies. In previous work we developed a series of 6-substituted-2-arylaminopurines that reversibly inhibited Nek2 (IC_{50} = 0.27–24 μM) and were selective (in some cases >10-fold *vs.* CDK2).[14] This work optimised interactions between the 2-arylamino group and the specificity pocket of the enzyme and revealed that basic or polar substituents *e.g.* tertiary amines, carboxamides, ureas and sulfonamides conferred good potency (*e.g.*, **8**; IC_{50} = 19 μM (Nek2)). The crystal structure of **8** in complex with Nek2 (Fig. 2A) revealed that the compound binds *via* a classical hydrogen bonding triplet between the purine N^9–H, N^3 and C^2–NH, and the main chain of kinase hinge region residues Cys89 and Glu87. Furthermore, the 6-alkoxy substituent was adjudged to be non-critical for binding affinity.[14] Closer inspection of the structure of the 2-arylamino-6-alkoxypurine **8** bound to Nek2 revealed that the P-loop cysteine (Cys22) is closely positioned to a putative superimposed 6-ethynyl (cyan) substituent (4.4 Å) (Fig. 2A). Moreover, the predicted angle of attack (74°) of cysteine SH at the terminus of the alkyne suggests that only a small realignment of the cysteine is required to achieve maximal orbital overlap with the alkyne π*. Hence, replacement of the 6-position substituent with an ethynyl group was expected to deliver an irreversible inhibitor (Fig. 2B).

Previous reports, including our model study,[15] have indicated that 6-ethynyl- and 6-vinyl-purines react *via* conjugate addition with nitrogen, oxygen and sulfur nucleophiles facilitated in part by the electron deficient purine.[16] Such compounds were also found to exhibit profound cytotoxicity in chronic myeloid leukaemia cell lines, which was postulated to arise by attack of nucleophilic amino acid residues on the electrophilic alkyne or alkene.[16a]

To build upon these foundations, a focussed series of derivatives was prepared that combined side chains known to confer potency in the competitive inhibitor class with a 'warhead' capable of covalently reacting with cysteine residues. The synthesis of 2-arylamino-6-ethynyl- and 6-vinyl-purines was therefore undertaken, along with appropriate control compounds, to explore their efficacy as irreversible Nek2 inhibitors and potential applications.

a) Synthesis of 6-ethynylpurine probe molecules

Initially, two 6-ethynylpurines bearing 2-arylamino groups were prepared (Scheme 1) as prototypes for irreversible inhibition of Nek2. Subjecting 2-fluoro-6-chloro-(9-tetrahydropyranyl)-purine (**10**)[17] to Sonogashira cross-coupling conditions afforded near quantitative yields of **11** when 3 mol% of $Pd(PPh_3)_2Cl_2$ and 2 mol% of CuI were employed with triisopropylsilylethyne (TIPS-ethyne, Scheme 1). The tetrahydropyranyl group was removed by acidic hydrolysis of **11** to give **12** (96% yield) as a central scaffold for further elaboration. Nucleophilic aromatic substitution (S_NAr) of the 2-fluoro substituent by aniline nucleophiles under previously established conditions[18] gave 2-arylamino-6-triisopropylsilylethynylpurines (**13**, **14**). The silyl group was removed by treatment with fluoride (either TBAF or KF with 18-crown-6) affording 2-arylamino-6-ethynylpurines **23** and **24**, albeit in a modest isolated yield. It was noted that if the TIPS moiety was removed from the ethynyl group at an earlier stage, then nucleophilic aromatic substitution at the 2-position of the intermediate purine failed to proceed.

To establish preliminary SARs at the 2-position, a series of compounds (**25–32**) was designed, bearing small alkyl, ether and halide substituents on the 2-arylamino ring, intended to probe the interaction of this structural element with the kinase. To avoid intractable reaction mixtures, potentially reactive heteroatoms (*e.g.* hydroxyl groups as in compound **18**) required protection (*e.g.* for hydroxyl, TIPS was used and removed concomitant with ethynyl group deprotection) prior to participation in the S_NAr step. In previous studies, carboxamides (*e.g.*, **8**) and sulfonamides (*e.g.* **9**) were generally found to afford the greatest Nek2 inhibitory activity and selectivity.[14] The scope of this study was therefore broadened through the synthesis of a number of more complex analogues derived from the corresponding anilines

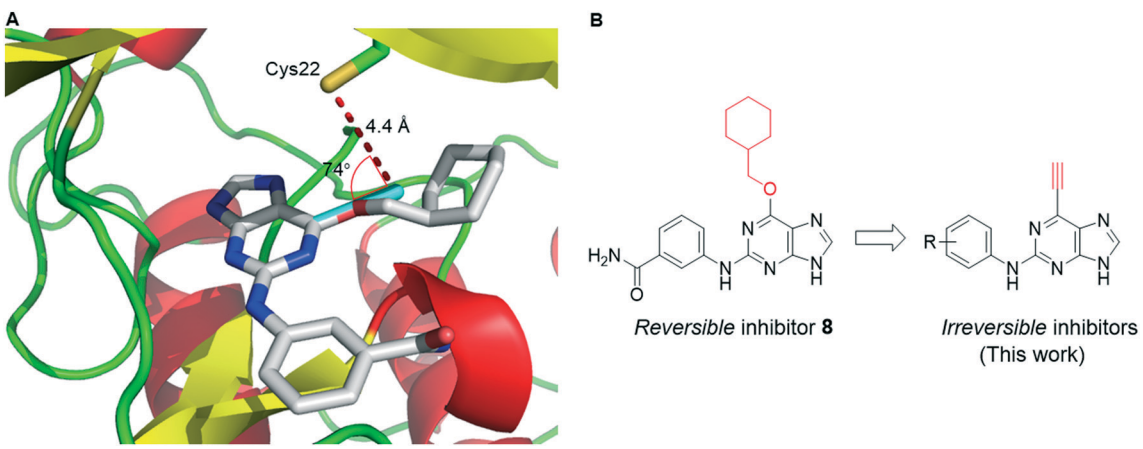

Fig. 2 A) X-ray structure (PDB code: 5 M51) of 2-arylamino-6-alkoxypurine **8** (grey) in complex with Nek2, superimposed with a putative 6-ethynylpurine (cyan) reveals that the alkyne is positioned for covalent interaction with cysteine 22. B) The proposed approach to deliver a covalently-reactive Nek2 inhibitor.

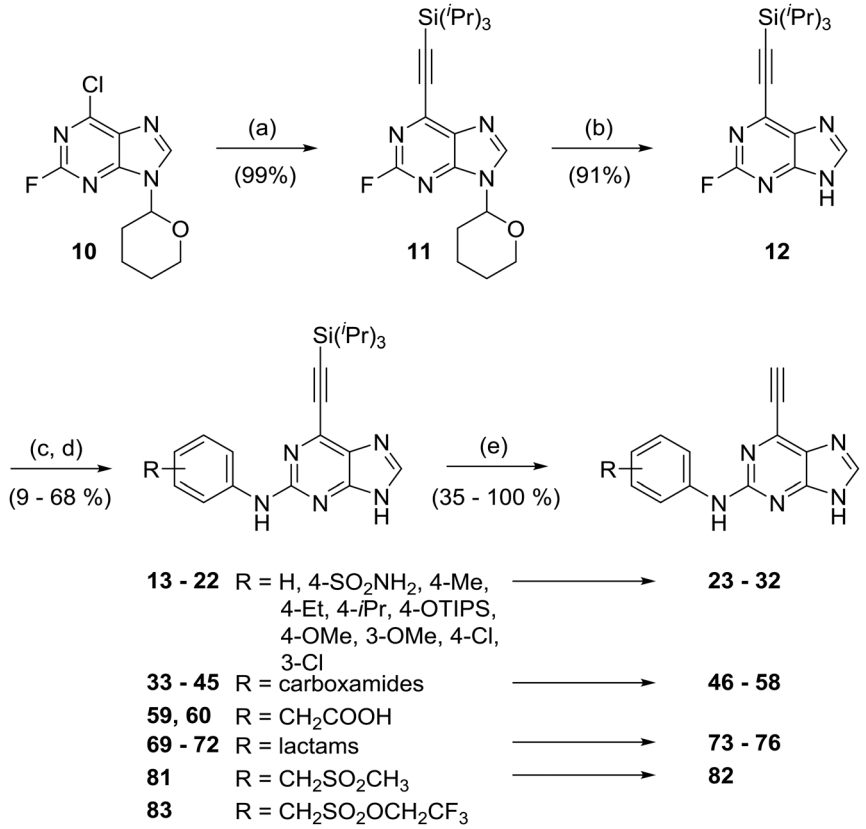

Scheme 1 General route to 6-ethynyl-2-arylaminopurines. Reagents and conditions: (a) triisopropylsilylacetylene, $Pd(PPh_3)Cl_2$, CuI, Et_3N, THF, RT, 18 h; (b) TFA, $^{i}PrOH$, H_2O, 100 °C, 2 h; (c) anilines, TFA, TFE, 80 °C, 18–27 h or MW 140 °C, 2 h; (d) TFA, reflux, 18 h (compounds **33** and **34**); (e) TBAF, THF, RT, 5 min or KF, 18-crown-6, THF, RT, 24 h.

(see ESI† for synthesis of the required anilines). Where necessary, coupling of 4-methoxybenzyl (PMB)-protected aminobenzamides to 2-fluoropurine (**12**) was followed by removal of the PMB-group using TFA at reflux prior to alkyne-deprotection (Scheme 1). This series of compounds allowed for possible additional interactions between *e.g.* basic groups of carboxamides (**46–58**) and the selectivity surface, which was previously found to confer higher potency and selectivity for Nek2 over other related kinases. This series included a carboxamide derivative (**58**) with a gem-dimethyl group.

Additional carboxamides were generated through coupling of 3- and 4-aminophenylacetic acid to 2-fluoropurine **12** under standard TFA/TFE-mediated conditions. This resulted in the formation of trifluoroethyl esters, which were hydrolysed under basic conditions to the required 3- or 4-substituted acids **59** and **60** without isolation (Scheme 1). The respective carboxylic acids were transformed into carboxamides **66–68** using 1,1′-carbonyldiimidazole (CDI) and the appropriate amine, followed by acidic deprotection of PMB-groups as required, and final removal of the silyl protecting groups (Scheme 2). To explore the consequences of conformational restrictions at the carboxamide side chain, a small series of purines bearing lactam groups (**73–76**) was prepared by the approach outlined in Scheme 1.

To probe the role of the carboxamide amino group of **66**, the ketone analogue **80** was synthesised. A modification of the Dakin–West reaction (conversion of an amino-acid into a ketoamide), can be used to convert a carboxylic acid with an enolisable carbon at the α-position into a methyl ketone. This method was employed to convert 3-nitrophenylacetic acid into 3-nitrophenylacetone by treatment with acetic anhydride in the presence of pyridine (modified Dakin–West reaction[19,20]). Protection of the carbonyl group of 3-nitrophenylacetone by conversion into a dithiane with 1,3-propanedithiol, was followed by reduction of the nitro group to afford aniline **77**. Coupling of **77** to the 2-fluoropurine **12** in the usual manner (Scheme 3) gave **78**. Stepwise removal of the dithiane (using [bis(trifluoroacetoxy)iodo]benzene) and silyl (TBAF) protecting groups furnished the target inhibitor (**80**) *via* intermediate **79**.

The homosulfonamide analogues of **24** probing the H-bond donor properties of the sulfonamide were prepared by either i) direct S_NAr reaction with the aniline according to Scheme 1, affording the sulfone **82**, or ii) from common intermediate, 2,2,2-trifluoroethylsulfonate ester **83** according to Scheme 4.[21] For the latter, reaction with amines in the presence of 1,8-diazabicyclo[5.4.0]undec-7-ene under microwave heating afforded sulfonamides in good to excellent yield.[21] Removal of all protecting groups was

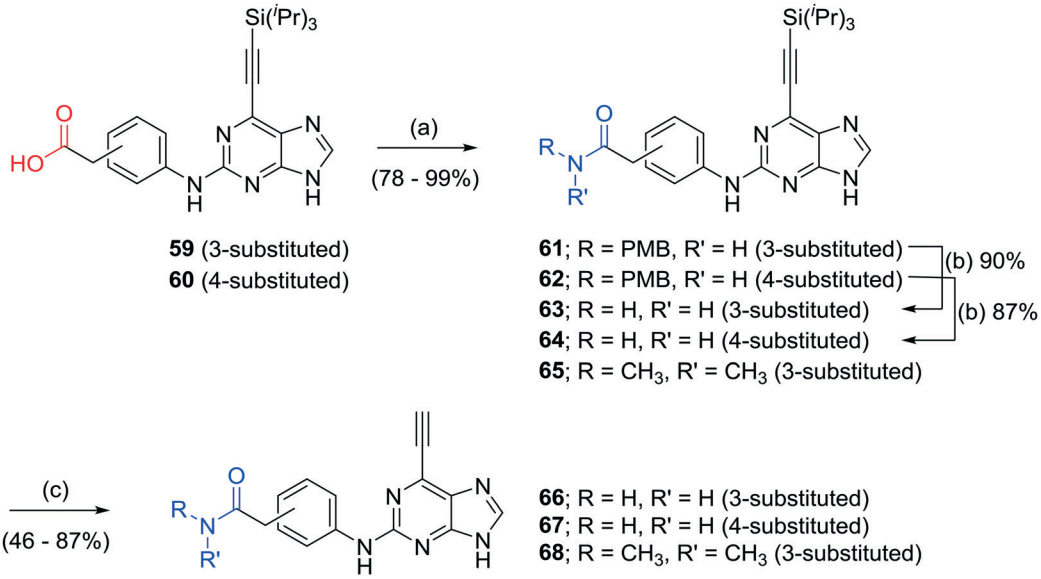

Scheme 2 Synthesis of carboxamide derivatives. Reagents and conditions: (a) i) 1 M NaOH, THF, RT, 18 h; ii) RNH_2, CDI, DIPEA, DMF, RT, 18 h; (b) TFA, reflux, 72 h; (c) TBAF, THF, RT, 5 min (followed in some cases by Amberlite 15 ion exchange resin, $Ca(OH)_2$, THF, RT, 48 h).

completed under the optimised conditions described above to give the target 6-ethynylpurines **87** and **88**.

The replacement of the 6-ethynyl group with a vinyl group was performed to probe the conformation of the conjugate acceptor within the binding pocket of Nek2 and to assess the potential for non-specific reactivity and toxicity. Initial attempts to synthesise the 6-vinylpurine analogues of **23** directly using a vinyltrifluoroborate salt and Suzuki–Miyaura coupling failed. 6-Vinylpurines have been prepared from thioethers by oxidation to the corresponding sulfoxide followed by base-induced elimination.[22] In our approach based on an earlier study,[23] to 6-vinylpurine (**92**) conjugate addition of homopiperidine to 6-ethynylpurine (**23**) furnished the enamine **89** (Scheme 5).[14,16d] Reduction[24] of **89** using sodium cyanoborohydride in the presence of 0.1 M HCl gave tertiary amine **90**. *N*-Oxidation of **90** using *m*-CPBA gave *N*-oxide (**91**), which underwent a Cope β-elimination[24] without heating, to give the desired 6-vinylpurine (**92**) in sufficient yield (30%).

b) Synthesis of control compounds

The 6-ethylpurine **96** was prepared as a control compound for comparison with the conjugate acceptor 6-ethynylpurine (**23**). 6-Ethynyl-2-fluoro-9-tetrahydropyranylpurine (**93**) was directly reduced with hydrogen in the presence of Lindlar's catalyst

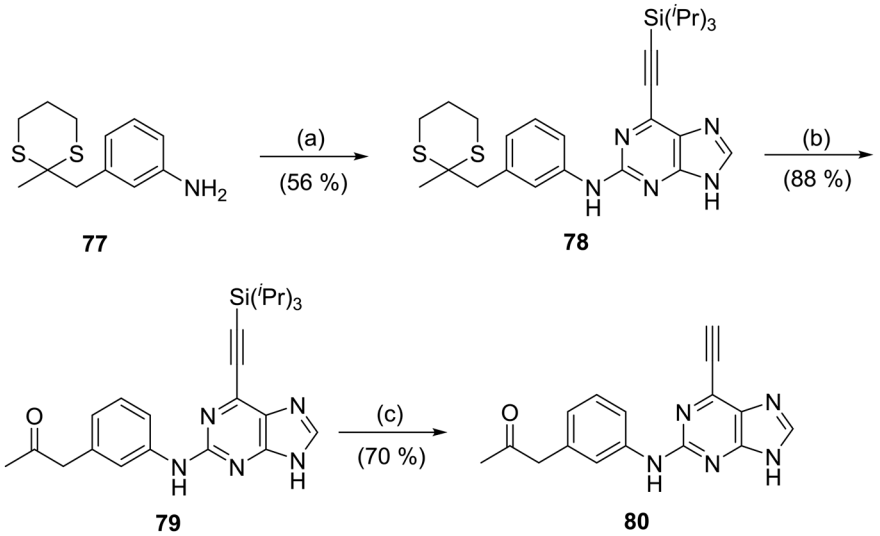

Scheme 3 Synthesis of sulfonamides. Reagents and conditions: (a) **12**, TFA, TFE, MW 140 °C, 2 h; (b) [bis(trifluoroacetoxy)iodo]benzene, MeOH, H_2O, RT, 10 min; (c) i) TBAF, THF, RT 5 min, ii) solid supported TBAF, THF, RT, 48 h.

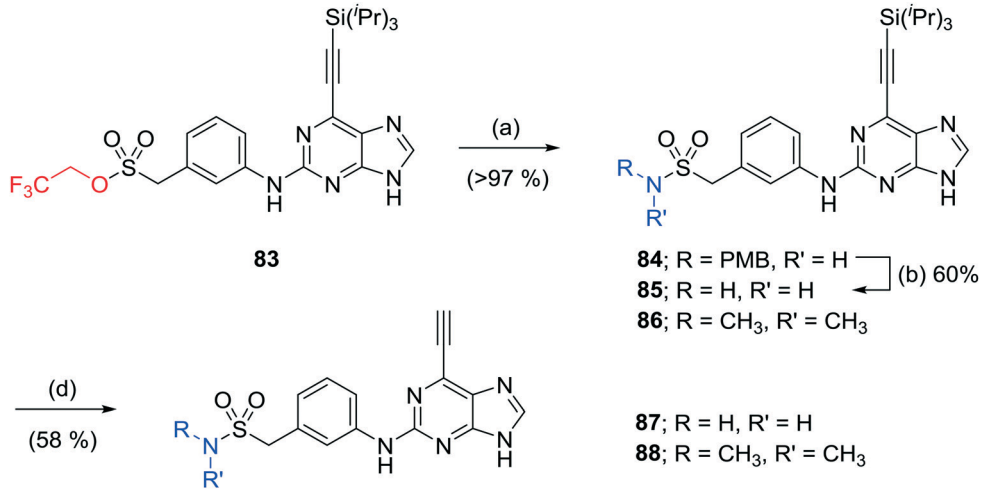

Scheme 4 Synthesis of sulfonamides. Reagents and conditions: (a) R_2NH, DBU, THF, MW 160 °C, 15 min; (b) TFA, 70 °C, 3 h; (c) TFA, DCM, RT, 18 h; (d) i) TBAF, THF, RT, 5 min, ii) Amberlite 15 ion exchange resin, $Ca(OH)_2$, THF, RT, 48 h.

with quinoline to the fully saturated 6-ethylpurine (**94**). The THP protecting group was cleaved by acidic hydrolysis followed by treatment with 4-aminobenzenesulfonamide under standard S_NAr conditions to produce **96** (Scheme 6).

6-Cyanopurine (**102**) was prepared by heating 2-bromohypoxanthine (**97**) with aniline to afford N^2-phenylguanine (**98**), which was converted into the 6-chloropurine **99**. The purine *N*-9/*N*-7 positions were protected as a ~3 : 1 mixture (*N*-9 : *N*-7) of 4-methoxybenzyl-substituted regioisomers. The major *N*-9-PMB isomer (**100**) was isolated in 52% yield and treated with Et_4NCN/DABCO to furnish cyanopurine **101**, from which the PMB group was removed in hot TFA (Scheme 7).

c) Biological evaluation of probes

i. 6-Ethynylpurines are irreversible inhibitors of Nek2. Initially, two simple 6-ethynylpurines, (**23** and **24**) were investigated as prototype irreversible inhibitors of Nek2, and exhibited encouraging and equivalent potency (Nek2 IC_{50} ~ 140 nM). Subsequently, a group of 2-arylamino-6-ethynylpurines (**25–32**) was prepared and showed good to moderate inhibition of Nek2 and that substitution at the 2-arylamino group was well tolerated. However, despite the variation in the substituent, there was only a modest variation in inhibitory activity (Fig. 3A) and little useful SAR understanding could be gained from this limited set of

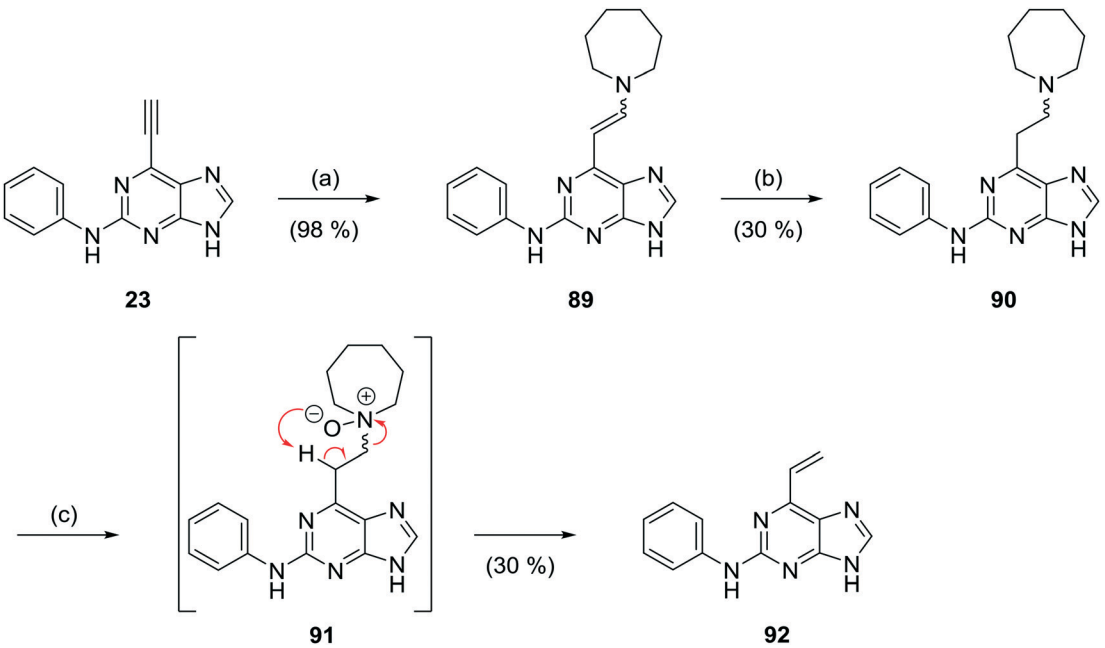

Scheme 5 *N*-Oxidation-β-elimination approach to 6-vinylpurine **92**. Reagents and conditions: (a) homopiperidine, THF, MW 100 °C, 10 min; (b) $NaBH_3CN$, TFA, THF, RT, 2 h, or $NaBH_3CN$, 0.1 M HCl, RT, 5 h; (c) *m*-CPBA, DCM, RT, 2 h.

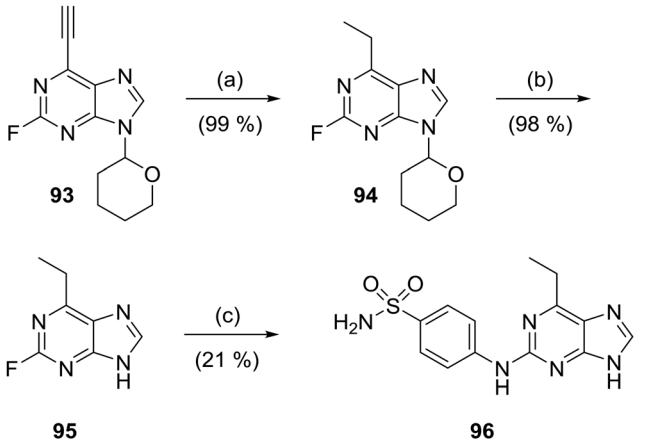

Scheme 6 Synthesis of 6-ethylpurine **96**. Reagents and conditions: (a) Lindlar's catalyst, quinoline, H_2, EtOAc, RT, 2 h; (b) TFA, 2-propanol, water, 100 °C, 2 h; (c) 4-aminobenzenesulfonamide, TFA, TFE, 90 °C, 48 h.

compounds. It should be noted that reporting inhibitory activity as IC_{50} may be inappropriate for irreversible inhibitors due to the time-dependence of the covalent reaction, although throughout this work activities are reported as IC_{50} after 30 min incubation with Nek2 unless otherwise stated.

Compounds **23** and **24** were selected as initial probes for determination of the mode of 6-ethynylpurine-mediated inhibition of Nek2. A kinase-inhibition reversibility assay (Fig. 3B) was employed to assess whether Nek2 pre-incubated with an inhibitor, *e.g.* **24** (30 min at 10 × IC_{50}, calculated to afford approximately 91% inhibition) could recover enzymatic activity upon rapid dilution (×100) of the enzyme–inhibitor complex with a solution containing ATP. Following this dilution, a reaction progress curve was generated by monitoring for levels of a phosphorylated substrate (Fig. 3B). Compound **24** afforded only approximately 3% recovery of activity, compared with 11% for a control competitive inhibitor, suggesting that 6-ethynylpurines are indeed covalent binders to Nek2. Further evidence was obtained through the confirmation of time-dependent inhibition of Nek2 kinase activity after treatment with **23** (Fig. 3C). To confirm whether time-dependent inhibition was mediated through Cys22, site-directed mutagenesis of this residue to alanine (Nek2-C22A) was performed, resulting in only weak competitive inhibition by **23** (IC_{50}, Nek2-C22A = 3.5 μM), with no increase in the degree of inhibition being observed with time of incubation (Fig. 3D).

ii. Selectivity profiling. To improve the confidence that Nek2 inhibition was responsible for observed cellular activity and to assess potential off-target enzyme inhibition, a panel of serine–threonine protein kinases was profiled against the ethynylpurines **23** and **24** (Fig. 3E). Despite evidence of modest Aurora A, CDK2, P70S6K and Chk2 inhibition, generally >10-fold selectivity for Nek2 was maintained. In agreement with earlier results, both **23** and **24** were poorly active against Nek1 (**23:** IC_{50} = 20.8 μM; **24:** 58% inhibition at 10 μM), which contains an alanine instead of the corresponding cysteine residue in Nek2, garnering further evidence of irreversible inhibition through cysteine-adduction. Importantly, selectivity was maintained over all seven other kinases tested (from a total of ten in the human kinome) that contain active-site cysteine residues: Rsk1,2,3; Msk1,2; Mekk1, Plk1 (ESI† Tables S1 and S2). Except for the cysteine, the residues that line the ATP binding pocket are divergent between these kinases and Nek2: the hinge sequences are different, only Nek2 and Plk1 share a Phe residue at the base of the pocket (Phe148 and Nek2). Of interest, Nek2 also has a cysteine residue in the hinge motif (Cys89) that could potentially be targeted with a covalent warhead, but almost 100 human kinases have an equivalent cysteine, and therefore this is not an attractive strategy to develop a selective inhibitor.

iii. Preliminary cellular evaluation. The 2-arylaminopurines **23** and **24**, were selected for further studies to investigate initial cellular effects of inhibitors within this class. Unfortunately, cellular growth-inhibition (U2OS, HeLa cell

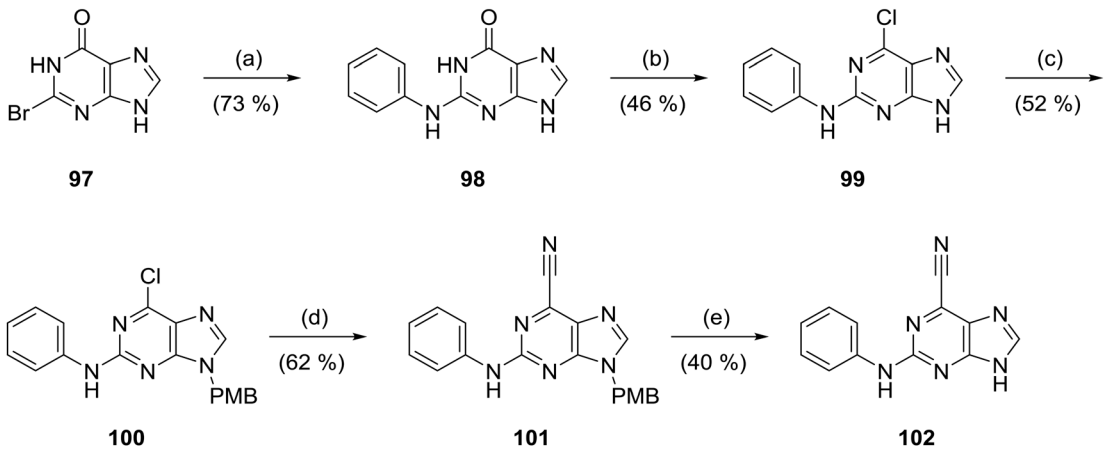

Scheme 7 Synthesis of cyanopurine **102**. Reagents and conditions: (a) aniline, TFA, TFE, 80 °C, 18 h; (b) $PhNMe_2$, $POCl_3$, 115 °C, 1 h; (c) 4-methoxybenzyl chloride, K_2CO_3, DMF, 60 °C, 18 h; (d) Et_4NCN, DABCO, MeCN, rt, 18 h; (e) TFA, 70 °C, 5 h.

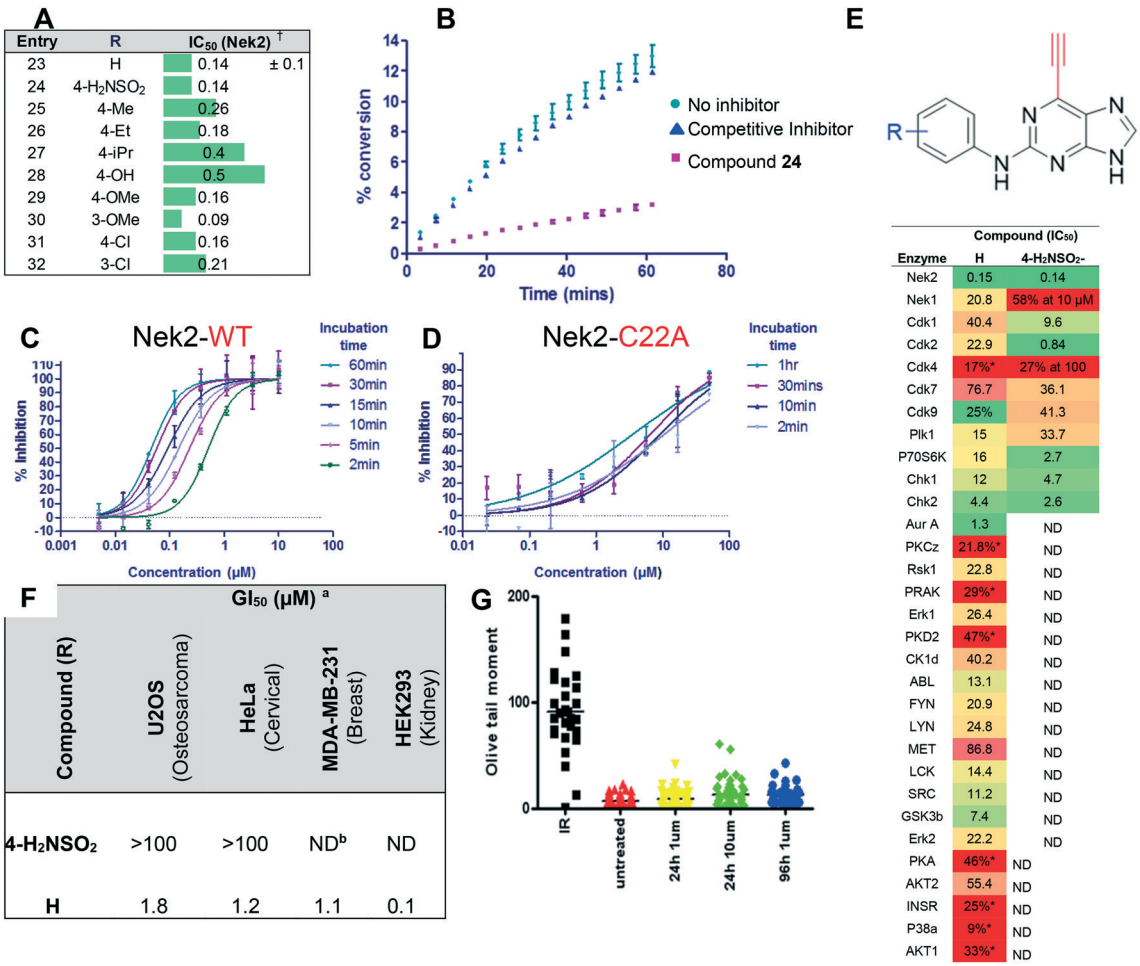

Fig. 3 Biochemical and cellular assessment of initial hit compounds **23** and **24** as irreversible inhibitors of Nek2: A) modification of the 2-arylamino motif. †Note: Nek2 IC_{50} values (uM) determined at 30 μM ATP concentration following a 30 minute incubation. B) Recovery of enzyme activity of Nek2 following dilution of the enzyme–inhibitor complex with ATP for **24** and a known ATP-competitive inhibitor of Nek2. C) and D) dose–response curves as a function of incubation time between **23** and Nek2-WT, and Nek2-C22A. E) Counter-screening of ethylnylpurines **23** and **24** against a panel of protein kinases (note: red = low inhibition, green = high inhibition). F) Cellular growth-inhibition by compounds **23** and **24** ([a] half maximal growth inhibitory concentration; [b] not determined). G) Comet assay results for cells treated with **23**.

lines) was found to be disappointing for **24**, which compared poorly with the cellular efficacy (U2OS, HeLa and MDA-MB-231 cell lines) observed for the parent phenyl compound **23** (Fig. 3F). This was tentatively attributed to the poor cell-permeability of the polar sulfonamide group of **24**. The growth inhibitory activity of phenyl derivative **23** in the HEK293 cell line (GI_{50} = 0.1 uM) raises the possibility of non-specific toxicity through action as a general electrophile, resulting in possible non-specific DNA or protein binding. Given the proposed mechanism of the 6-ethynylpurine inhibitors, it was considered that they could act as DNA alkylators *via* a similar mechanism. In order to determine the effect of treatment with the inhibitor on cellular DNA damage, a Comet assay was performed (Fig. 3G). MDA-MB-231 breast cancer cells were treated with **23** for up to 96 h and displayed similar olive tail moments to untreated cells, confirming that DNA damage is not a major effect of this inhibitor class.

Given the observed cellular activity and apparent selectivity for Nek2 over other kinases, 6-ethynylpurine **23** was considered a suitable starting point from which to conduct modification to further improve inhibitor potency. According to our previously reported findings,[14] Nek2 competitive inhibitors of the 6-alkoxypurines class bearing a basic group at the 2-arylamino ring were found to confer good potency and cellular activity. It was considered that this would translate to the irreversible inhibitors class as the competitive binding phase was crucial to achieving targeted and potent inhibition. The parent 6-ethynylpurine irreversible inhibitor (**23**) was modified at the 2-arylamino to produce a series comprising carboxamides (**46–58**, **66–68**, **73–76**) and sulfonamides (**87** and **88**), which were screened for inhibitory activity against Nek2 (Table 1). In addition, 6-ethynylpurines were evaluated for growth inhibitory activity *in vitro* against the SKBR3 tumour cell line.

All purine derivatives tested exhibited inhibitory activity against Nek2 with all but compound **74** possessing an IC_{50} of

less than 0.13 μM. It is evident that the activity of the parent 3-substituted carboxamide **66** (IC_{50} = 0.062 ± 0.01 μM) is not affected by truncation (**46**, IC_{50} = 0.116 μM) or homologation (**47**, IC_{50} = 0.079 μM) of the methylene spacer group. Reversing the carboxamide (**57**, IC_{50} = 0.039 μM) and complete removal of the heteroatom, through synthesis of ketone **80** (IC_{50} = 0.076 μM) were inconsequential modifications. Furthermore, moving the 2-arylamino ring substituents from the 3- to the 4-position (*e.g.*, **67**; IC_{50} = 0.093 μM) had little influence on the measured enzyme inhibition. Sequential removal of the carboxamide hydrogen atoms through *N*-methylation, affording *N*-methylcarboxamide (**48**, IC_{50} = 0.076 μM) and *N*,*N*-dimethylcarboxamide (**68**, IC_{50} = 0.088 μM) analogues of **66** had little effect on Nek2 inhibitory activity, which was true for both 3- and 4-substituted carboxamides.

Conformational restriction of the carboxamide motif appeared to be somewhat detrimental, with gem-dimethyl carboxamide **58** (IC_{50} = 0.21 μM) exhibiting a small, approximate 3-fold reduction in inhibitory activity. Moreover, it is likely that the conformational restriction imposed by a bicyclic 2-arylamino system either disrupts favourable or promotes unfavourable interactions within the ATP-binding site of Nek2, as exemplified by compound **74** (IC_{50} = 0.82 μM). This suggests that the optimal 2-arylamino side-chain characteristics are more linear with respect to the purine scaffold, as indicated by comparison of the activity of **74** with that of the regioisomeric analogue **73** (IC_{50} = 0.10 μM). In contrast to the carboxamide examples, the *N*,*N*-dimethylsulfonamide analogue (**88**, IC_{50} = 0.010 μM) lacking an H-bond donor atom conferred a significantly improved potency when compared with the primary sulfonamide (**87**, IC_{50} = 0.130 μM). However, this may be simply a function of physicochemical properties *e.g.*, solubility.

Within this compound class, only rather limited SARs are evident, with no discernible trend observed between the activity of compounds against Nek2 and the degree and/or nature of modification of the carboxamide group. Presumably, all compounds excluding **74** exhibit sufficient initial competitive binding affinity for Nek2 to allow the purine to occupy the ATP-binding domain of the kinase and enable subsequent covalent modification of Cys22 to occur. The weaker activity observed for **74** does suggest that it is possible to elucidate SARs for this compound class and that potent activity is not common to all of the 6-ethynylpurines. What these data do reveal, however, is that for irreversible inhibitors in the 6-ethynylpurine class, there is a large degree of tolerance for substitution on the 2-arylamino ring. This indicates that significant structural changes should be tolerated in order to enhance pharmacokinetic/physicochemical properties yet may promote concerns of potential off-target toxicity. Coupled with this, all compounds detailed in Table 1 exhibited growth inhibitory activity in the SKBR3 cell line, yet there appeared to be a poor correlation between the IC_{50} of compounds in the Nek2 kinase assay and their activity in the SKBR3 cellular GI_{50} assay. In particular, compound **74** (Nek2; IC_{50} = 0.82 μM, SKBR3; GI_{50} = 1.3 ± 0.2 μM) was the least active inhibitor in the Nek2 assay, but proved one of the more potent growth inhibitors in SKBR3 cells. Off-target inhibition or non-specific toxicity are common challenges to overcome within protein kinase inhibitor design, and in particular for irreversible inhibitors. As such, it was considered that these may play a role in the conflicting cellular *versus* enzyme activity data, despite the promising Comet assay data obtained for **23**.

Whilst the carboxamide derivative **66** was identified as amongst the most potent inhibitors in this class and inhibited growth of SKBR3 cell lines (Table 1), the improvement in kinase inhibitory activity did not correlate with the cellular growth inhibitory activity observed in U2OS and HeLa (Table 2) cell lines. It was possible that this was again a consequence of the more polar nature of the 2-arylamino side-chain limiting cellular permeability.

Owing to concerns over lack of kinase selectivity of this compound class, the inhibitory activity of **66** was profiled against a panel of 48 kinases selected from commercially available ProfilerPro® plates at 1 μM inhibitor concentration (see ESI,† Table S1). Only two kinases other than Nek2 were inhibited by greater than 50%, and IC_{50} values were determined for these: Aurora A (IC_{50} = 0.08 μM) and BMX (IC_{50} = 0.83 μM). It is notable that BMX kinase, a member of the EGFR tyrosine kinase family, possesses a cysteine residue within the ATP-binding domain that has been identified as a potential target in the design of irreversible inhibitors.[25] In addition, both **23** and **66** were screened against 121 kinases (National Centre for Protein Kinase Profiling, Dundee University) at a single concentration of 1 μM (see ESI,† Table S2). Greater than 50% inhibition of activity was observed for nine of the kinases tested by **66**, including Nek2, and IC_{50} values were determined (Table 3). Encouragingly, the IC_{50} of **66** against Nek2 was 18 nM in this assay, giving the compound at least 5–10-fold selectivity for Nek2 over other kinases, whilst AurA was only weakly inhibited by **66** in this screen.

Interestingly, **23** displayed a better overall selectivity profile for Nek2 compared with **66**. In addition to Nek2, only two other kinases (MLK3 and TAK1) were inhibited by greater than 50%. It is possible that the alternative target responsible for the cellular activity of **23** is not included in the screen, which constitutes only a fraction of the human kinome. Conversely, the locus of cellular activity for **23** may not be a kinase.

In keeping with the ultimate objective of developing a targeted therapy, **66** was screened for cell growth inhibition (10 μM, 72 h) against a panel of cell lines to identify specific tumour types where depletion of Nek2 activity is growth inhibitory (Fig. 4A–C). Previous findings in this area indicated that cell lines derived from breast tumours and leukaemias may be particularly sensitive to pharmacological Nek2 inhibition. As was observed previously, the tumour cell lines most sensitive to inhibitor treatment were those derived from breast (MCF7, T47D, ZR75, SKBR3 and MDA-468) and

Table 1 Examples of 2-arylamino-6-ethynylpurines synthesised and studied in this work

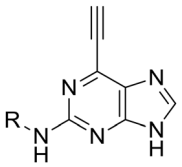

Compound	R	IC_{50} (μM) Nek2[a]	GI_{50} (μM) SKBR3
46	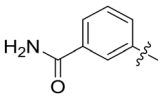	0.116	0.7 ± 0.1
47	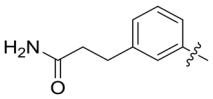	0.079	3.9 ± 1.3
48	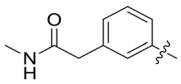	0.076	2.4 ± 0.1
49	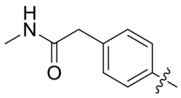	0.072	4.9 ± 2.4
50	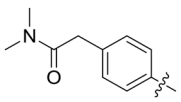	0.057	1.2 ± 0.6
51	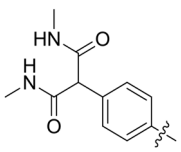	0.071	87.8
52	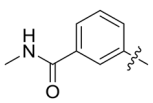	0.026	0.9 ± 0.1
53	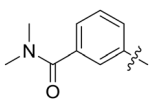	0.050	0.9 ± 0.1
54	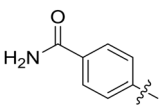	0.110	7.4 ± 0.1
55	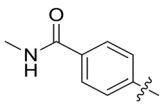	0.110	4.1 ± 0.5
56	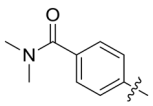	0.064	1.4 ± 0.4
57	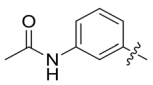	0.039	0.8 ± 0.5
58	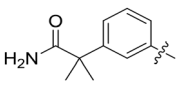	0.210	1.4 ± 0.6
66	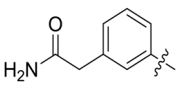	0.062 ± 0.01	2.2 ± 0.4
67	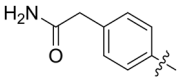	0.093	8.8 ± 1.8

Table 1 *(continued)*

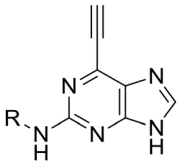

Compound	R	IC_{50} (μM) Nek2[a]	GI_{50} (μM) SKBR3
68	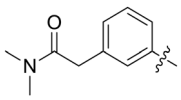	0.088	0.4 ± 0.2
73	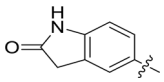	0.100	10.3
74	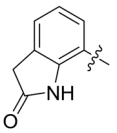	0.820	1.3 ± 0.2
75	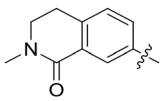	0.010	—
76	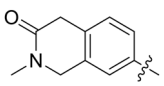	0.042	0.8 ± 0.1
80	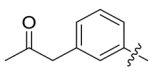	0.076	—
82	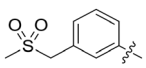	0.057	1.3 ± 0.0
87	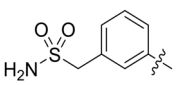	0.130	4.1 ± 2.2
88	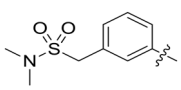	0.010	—

All IC_{50} values are results obtained from n = 3 determinations. [a] Nek2 IC_{50} values determined at 30 μM ATP concentration following a 30 minute incubation.

leukaemia (Rec-1 and RIVA), with all of these cell lines exhibiting greater than 50% growth inhibition at a dose of 10 μM **66**. GI_{50} values were determined for these cell lines, along with HeLa and HCT116 (Fig. 4D and E), with the lymphoma Rec-1 (GI_{50} = 1.6 ± 0.1 μM) and breast cancer SKBR3 (GI_{50} = 2.2 ± 0.4 μM) cell lines being identified as particularly sensitive to **66** treatment. Furthermore, **66** was also found to be cytotoxic in SKBR3 cells; clonogenic assays with this cell line gave LC_{50} values in the low micromolar range following pre-incubation for as little as 3 hours prior to subculture (Fig. 4F).

iv. C-Nap1 as a cellular biomarker for Nek2 inhibition. To confirm that cellular Nek2 is inhibited upon treatment with the ethynylpurines, *e.g.* **23**, a cellular biomarker was required. The phosphorylation state of C-Nap1 localised to the centrosomes was used. As C-Nap1 is a substrate only for Nek2, this can be used as a direct measure of cellular Nek2 activity. Encouragingly, cells treated with **23** displayed inhibition of C-Nap1 phosphorylation levels to approximately 20% of control at doses of 1 × GI_{50} (1.8 μM) (Fig. 5A), indicating that cellular permeability was not a problem. Despite showing negligible inhibition of cell growth, cells treated with **66** have pC-Nap1 levels reduced to a comparable degree at 0.07–0.14 × GI_{50} (5.0–10.0 μM). This strongly suggests that growth inhibition observed in U2OS cells following exposure to **23** arises *via* an alternative target. Cellular growth inhibition was not evident for **66**, presumably owing to improved compound selectivity.

v. Structural biology confirms covalent binding of ethynylpurines. To examine the binding mode of ethynylpurines to Nek2 and observe the covalent bond directly, we solved X-ray co-crystal structures of Nek2 with compounds **24** and **66**, and also with the competitively-binding control compounds **96** and **102** (see ESI,† Table S3). C-Terminally his-tagged Nek2 1-273 protein was expressed, purified and crystallized as previously described.[26] Crystals of

Table 2 Enzyme *versus* cellular inhibitory activity of unsubstituted (**23**), homocarboxamide (**66**) and homosulfonamide (**87**) 2-arylamino-6-ethynylpurines

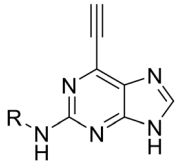

Compound	R	IC_{50} (μM) Nek2[a]	GI_{50} (μM) U2OS	GI_{50} (μM) HeLa
23	Ph	0.14 ± 0.1	2.1 ± 1.0	1.2 ± 0.5
66	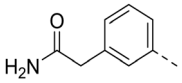	0.062 ± 0.01	71.0	47.1 ± 2.1
87	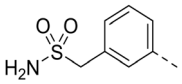	0.13	N.D.	N.D.

All IC_{50} values are results obtained from n = 3 determinations. [a] Nek2 IC_{50} values determined at 30 μM ATP concentration following a 30 minute incubation; N.D. not determined.

Table 3 IC_{50} values for kinases inhibited by **66** by greater than 50% in the National Centre for protein kinase profiling screen. Colour code: green (relatively potent inhibitor), red (relatively weak inhibitor)

Kinase	Nek2	MKK1	MLK1	MLK3	NUAK1	TBK1	TAK1	JAK2	Chk1
IC_{50} (μM)	0.018	0.55	0.27	0.32	0.12	0.74	0.24	0.22	0.56

inhibitor-bound Nek2 were generated by soaking ADP-bound Nek2 crystals in mother-liquor supplemented with each of the inhibitor compounds for several hours before cryo-protection and cryo-cooling. Diffraction data were collected at Diamond Light Source and ESRF and X-ray crystal structures were solved by molecular replacement and refined as previously described.[26] The structure of Nek2 in complex with the 6-ethynylpurine **24** was solved to 2 Å resolution (Fig. 6A) and revealed that the triplet of hydrogen bonds between the purine and the kinase hinge region (Cys87 and Glu87) is maintained in an almost identical binding mode to the previously reported reversible binding class of 6-cyclohexylmethoxypurines. Having established that the ethynyl motif present in **23** and **24** may be responsible for covalent adduction, the cysteine residue (Cys22) present in the catalytic domain of Nek2 was found to be well positioned for the proposed conjugate addition to the bound inhibitor. Furthermore, crystal structure analysis (Fig. 6B) clearly showed a covalent bond between the sulfur of Cys22 and inhibitor **24**, supporting the mechanism of irreversible modification proposed in Fig. 6D. X-ray crystallographic analysis confirmed that **66** also bound to the Nek2 ATP-binding site in the expected manner, with covalent modification of Cys22 evident (Fig. 6C). Potential interactions between the carboxamide side-chain of inhibitor **66** and the carboxylic acid side-chain of Asp93 were also identified (Fig. 6C), suggesting that it should be possible to attain greater binding-affinity through appropriate substitution at the 2-arylamino-group. It may be that the hinge interaction is also crucial for activation of 6-ethynylpurines towards nucleophiles, by partial protonation of N-3 of the purine which accepts a hydrogen bond upon binding. The terminal alkyne should consequently be more susceptible to a Michael-type addition by an active site nucleophile (*e.g.*, Cys-SH, Fig. 6D). It is likely that the conjugate addition proceeds *via* an allene intermediate that tautomerises to afford a thioenol-ether adduct.

vi. Evaluation of control compounds. To dissect the role of the covalent binding ethynyl group from the putative initial reversible binding 2-arylaminopurine, a series of ethynyl group-replacements were introduced at the 6-position of **23** and **24**. In each case, control compound **92**, **96** and **102** that were predicted to make the same interactions with the kinase active-site, but lack the covalent modifying ethynyl functional group, exhibited significantly lower inhibitory activity in biochemical assays making them important tool compounds (Table 4).

Perhaps the most intriguing result was related to the 6-vinylpurine **92**, which is reported to undergo conjugate addition reactions with thiols, albeit at a slightly slower rate than 6-ethynylpurines.[15] **92** was found to be a very weak Nek2 inhibitor (17% inhibition at 10 μM) compared with ethynyl analogue **23** (IC_{50} = 0.14 μM). This indicates that the geometry of the conjugate-acceptor substituent at the purine

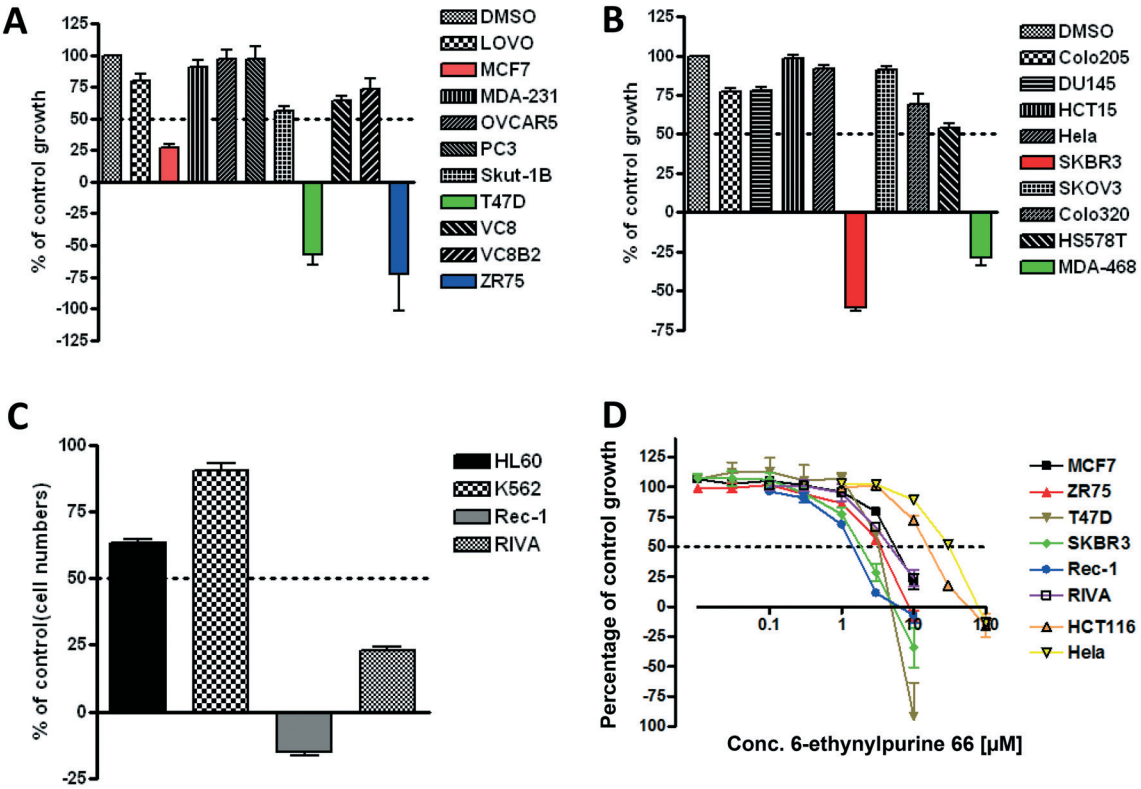

E

Cell Line	MCF7	ZR75	T47D	SKBR3	Rec-1	RIVA	HCT116	HeLa
GI_{50} (μM)	6.6 ± 0.9	3.7 ± 0.8	3.6 ± 0.5	2.2 ± 0.4	1.6 ± 0.1	5.8 ± 1.4	18.1 ± 1.6	32.2 ± 3.9

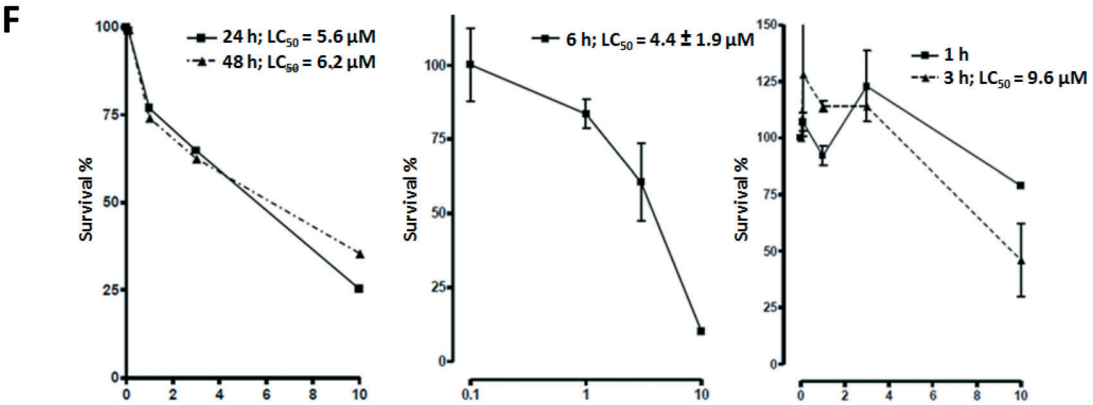

Fig. 4 A) Growth inhibition of solid tumour cell lines treated with 10 μM **66** for 72 hours. B) Growth inhibition of solid tumour cell lines treated with 10 μM **66** for 72 hours. C) Growth inhibition of leukaemia cell lines treated with 10 μM **66** for 72 hours. D and E) Growth inhibition of cell lines identified as being sensitive to **66** following 72 h exposure to inhibitor (n = 3). F) Cytotoxicity of **66** in SKBR3 cells following incubation for a range of times.

6-position is critical, underlining the importance of correctly aligning the conjugate acceptor group with Cys22. However, it is possible that due to lower thiol-reactivity, **92** requires a longer incubation time within the Nek2 active site to be equipotent with **23**. This outcome is of critical importance and alleviates the fear that unwanted side-reactions would occur indiscriminately.

The saturated 6-ethylpurine (**96**) is a non-conjugate acceptor, lacking an alkene/alkyne purine 6-substituent required for Michael-type addition reactions. Compound **96** was found to be a weak inhibitor of Nek2 (IC_{50} = 46.8 μM), but was shown to bind in an identical orientation in the Nek2 active-site as the 6-ethynyl derivative **24** (Fig. 7). The crystal structure of Nek2-**96** complex superimposed with

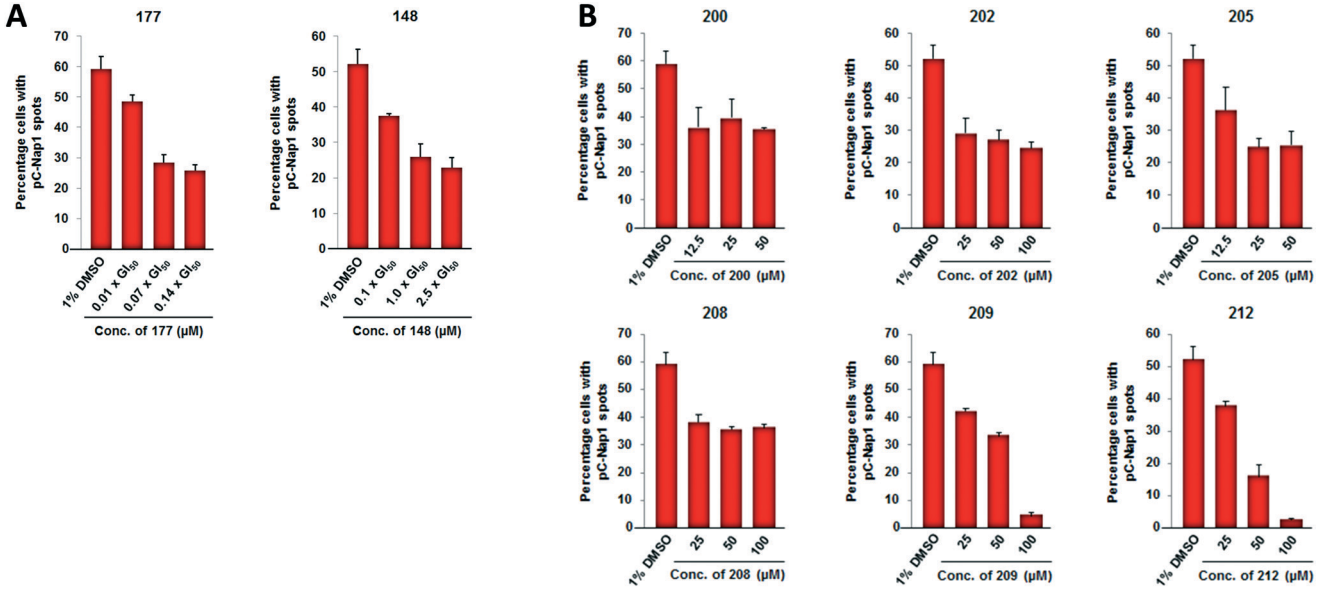

Fig. 5 A) Inhibition of C-Nap1 phosphorylation in U2OS cells by **66** compared with **23**. B) Dose-dependent reduction of pC-Nap1 levels for selected carboxamides within the 6-ethynylpurine series.

Nek2-**24** (Fig. 7) revealed that the covalent link between **24** and Cys-22 of Nek2 is accompanied by a relative movement of the N-terminal lobe towards the C-terminal lobe. This movement of the N-terminal lobe is not evident when the competitive inhibitor (**96**) is in complex with Nek2.

The nitrile group of **102** retains both the linear geometry of the ethynyl group is not expected to undergo conjugate addition by nucleophiles such as thiols in the same manner as 6-ethynylpurines. **102** was measured to be a weak competitive inhibitor of Nek2 (IC_{50} = 12 μM) and was approximately 200-fold less potent against Nek2 than the equivalent 6-ethynylpurine (**23**). This result suggested that the competitive binding component only contributes weakly to the activity observed in the 6-ethynylpurine series, assuming that **23**, **24** and **102** make similar binding interactions with Nek2. Superposition of the crystal structure of **102** in complex with Nek2 confirmed that a near identical binding-orientation arose compared with the benchmark 6-ethynylpurine **24** (Fig. 8A). The covalent adduction of **24** can clearly be seen by the thioenol ether formed between **24** and Cys22. This is absent in the crystal structure of the cyano compound, indicating that no covalent interaction arose although the same mode of binding of the shared scaffold into the nucleotide-binding pocket of Nek2 was observed and the triplet of hydrogen bonds between the purine and the kinase hinge motif was preserved (Fig. 8B and C). Significantly, *in vitro* growth inhibition assays showed that **102** ($GI_{50} > 100$ μM) has no effect on cell viability in three human tumour cell-lines, WT U2OS, MDA-MB-231 and HeLa cells, as well as in the 'normal' human embryonic kidney (Hek293) cell-line.

vii. *In vitro* pharmacokinetics of 6-ethynylpurines. Further studies to characterise **66** were undertaken, including preliminary *in vitro* ADME testing (Cyprotex Discovery, Macclesfield, UK) (Table 5). These studies suggested that **66** possessed the attributes of a drug-like compound. The purine was found to have good aqueous solubility, no inhibition of hERG (human ether-a-go-go-related gene product) was observed at 25 μM, and **66** exhibited a good stability profile in both human and mouse liver microsomes, despite the electrophilic 6-ethynyl group, probably reflecting the low lipophilicity of the compound (cLogP = 1.4). Studies employing the Caco-2 cell line allowed an estimation of compound permeability and efflux to be determined. The direction [A → B] equates to compound passing from the gastrointestinal tract into the blood, with [B → A] relating to drug efflux in the reverse direction. The inhibitor showed low permeability and high efflux, suggesting that the oral bioavailability of **66** may be poor. It is possible, however, that the inherent permeability of the compound is good, but that it is also a substrate for drug efflux transporters.

***In vivo* modelling.** The promising *in vitro* results prompted the evaluation of **66** in *in vivo* models for both pharmacokinetics (PK) and antitumour efficacy. In a preliminary PK evaluation, **66** was administered at a single dose to female CD1 mice. The compound was rapidly cleared from the blood following intravenous administration, with a low area under the curve (AUC), high clearance and a short half-life ($T_{1/2}$). No inhibitor was detected in blood samples for animals treated orally. Compound **66** has poor permeability and is readily effluxed in the Caco-2 model which translates into poor oral bioavailability due to poor absorption. To understand the rapid clearance of **66**, stability studies were performed for the compound in buffered solutions at pH 2, 7.4 and 10, and in a solution containing 5 mM glutathione (GSH), which approximates to intracellular concentrations. Samples of **66** in the three solutions were incubated at 37 °C and the concentration of **66** determined by HPLC at time points over 18 h. It is likely that **66** is poorly soluble in

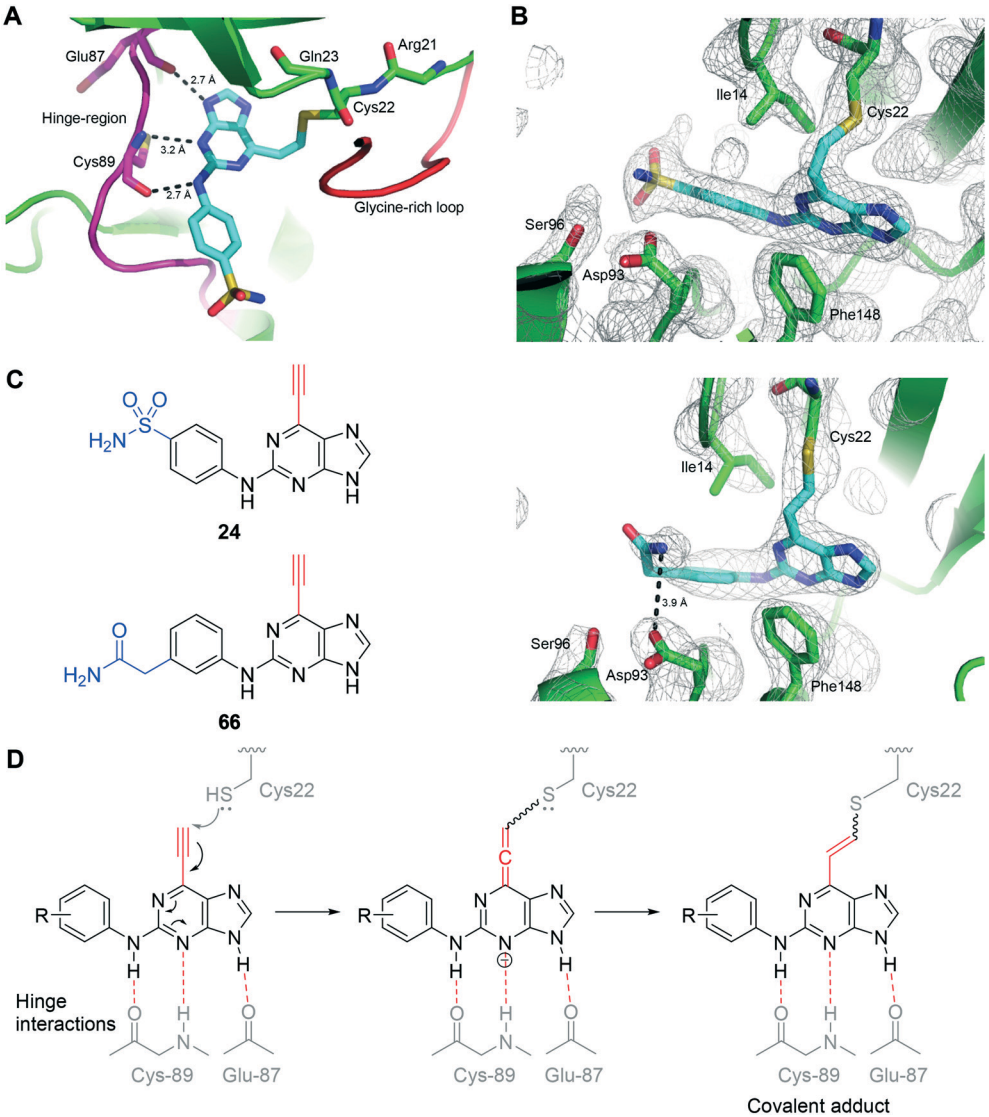

Fig. 6 Interaction of irreversible inhibitors **24** and **66** with Nek2: A) crystal structure of **24** (cyan) bound to Nek2 indicating interactions with the hinge-region of the kinase (pink) and B) crystal structure of Nek2 (green) in complex with **24** (cyan) including electron density map (2Fo-Fc) contoured at 1.0σ (mesh). C) Crystal structure Nek2 (green) in complex with **66** including electron density map (2Fo-Fc) contoured at 1.0σ (mesh). A potential interaction with the side chain of Asp93 is indicated. D) Proposed mechanism of covalent adduction of cysteine-22 by ethynylpurines.

solutions at higher pH, and therefore the concentration only becomes consistent once the sample is incubated at 37 °C for 10 minutes. It was evident that under the assay conditions, **66** is consumed in a time dependent manner in the presence of glutathione. This suggests that reaction with glutathione may contribute to the rapid clearance observed for **66**. Notwithstanding the reactivity of compound **66** with glutathione, in the mechanistic cellular C-Nap1 assay activity was nonetheless observed with a number of compounds, and therefore instability in the presence of glutathione at physiological concentrations does not preclude cellular activity.

Conclusions

Achieving selectivity between specific members of the same or closely-related protein kinase families is challenging owing to the high degree of structural homology within the catalytic domain. However, targeting specific nucleophilic residues close to the catalytic site provides a means to discriminate. In this context, it is therefore encouraging that over 200 protein kinases contain a targetable cysteine residue close to the catalytic site.[2,27–29] Covalent binding of an enzyme inhibitor has the potential advantages of prolonged duration of action and enhanced pharmacological efficacy, which allows lower dosing and reduced off-target effects. However, this advantage may not be relevant for Nek2 protein, which has a short cellular half-life of 45–75 minutes.[30] There is concern that covalent binding agents will exhibit non-specific activity and off-target toxicity (*e.g.* promotion of immune responses[31]) owing to their perceived ability either to react almost randomly with biological nucleophiles, *e.g.* proteins and nucleic acids, or to be quenched by glutathione.

Table 4 Replacement of the ethynyl covalent-acceptor motif

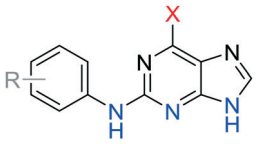

Compound	R	X	IC_{50} (Nek2)[a]
23	H		0.145 μM
24			0.140 μM
92	H		17% at 10 μM
96		Et	46.8 μM
102	H		12 μM

All IC_{50} values are results obtained from $n = 3$ determinations.[a] % inhibition or IC_{50} determined after 30 min.

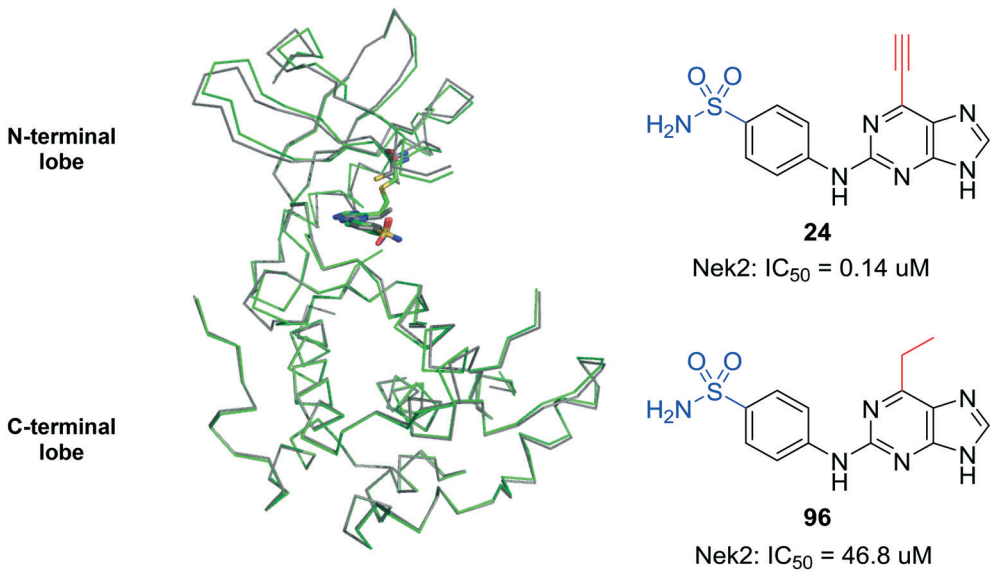

Fig. 7 Overlay of the ATP-binding domain of Nek2 in complex with **24** (green) and **96** (grey).

However, this belief ignores the strict stereoelectronic requirements for efficient reaction of a protein nucleophile with an electrophilic reagent,[15] and thus so far adverse properties of covalent inhibitors have been found to be minimal. Nevertheless, the development of covalent inhibitors must recognise the potential for off-target effects and be biomarker-focussed throughout. In this paper we have shown that selective covalent binding to Nek2 can be achieved with ethynylpurines, which exhibit numerous positive features as potential anticancer agents and therefore provide ample justification for the pursuit of this protein target with small molecule inhibitors.

Experimental section

Chemicals and solvents

All chemical reagents were purchased from the Aldrich Chemical Company, Apollo Scientific or Alfa Aesar Chemicals and were of the highest available purity. Chemicals were used as supplied with no further treatment. If chemicals used were stated as dry/anhydrous, they were stored in SureSeal™ septum-sealed bottles and removed under an inert nitrogen environment, with the reaction being carried out under the relevant inert atmosphere. Palladium catalysts were stored and measured out under an inert atmosphere.

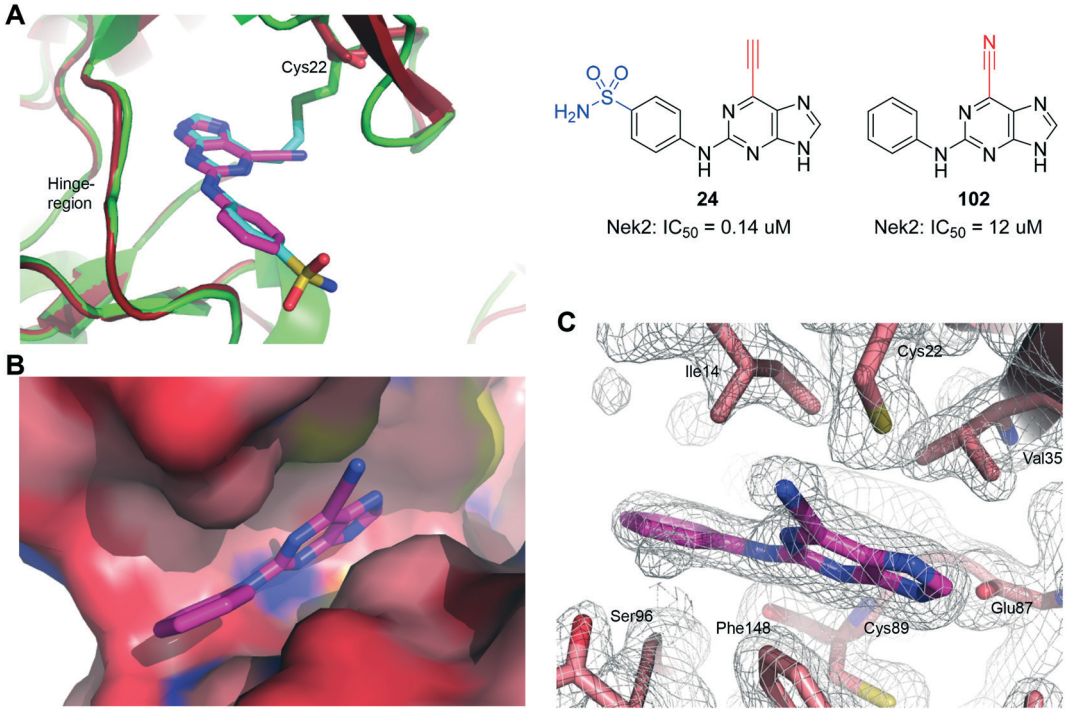

Fig. 8 Interaction with competitively binding control compound **102** with Nek2: A) alignment of crystal structures of Nek2 (green) covalently bound to **24** (cyan) and Nek2 (red) non-covalently bound to **102** (magenta). B) Space-filling representation of **102** (magenta) bound into the nucleotide-binding pocket. C) Crystal structure of **102** (magenta) bound to Nek2, including electron density map (2Fo-Fc) contoured at 1.0σ (mesh). Hydrophobic residues lining the pocket, the hinge residues Glu87 and Cys89, and unadducted Cys22 are indicated.

Table 5 *In vitro* ADME properties for **66** (Cyprotex Discovery, Macclesfield, UK)

Microsomal stability							
Microsomal stability (human)				Microsomal stability (mouse)			
CLint (μL min^{-1} mg^{-1})	S.E. CLint	$T_{1/2}$ (min)	n	CLint (μL min^{-1} mg^{-1})	S.E. CLint	$T_{1/2}$ (min)	n
6.21	0.681	223	5	10.2	1.82	136	5

Solubility		
Estimated precipitation range (μM)		
Lower bound	Upper bound	Calculated mid-range
100	>100	>100

Caco-2 permeability						
	Papp (× 10^{-6} cm^{-1})		Mean Papp (× 10^{-6} cm^{-1})	SD	n	Mean recovery (%)
Direction	1	2				
A → B	0.0534	0.0421	0.0477	0.00799	2	57.6
B → A	4.88	5.29	5.08	0.293	2	64.0

Chromatography

Reaction monitoring and compound identification was aided using thin layer chromatography (TLC) and retardation factor (R_f) values. TLC was conducted with Merck aluminium backed Si F_{254}, NH_2 F_{254s} and RP-18 F_{254s} plates. Fluorescent compounds were visualised under short wave (254 nm) UV irradiation. Compound purification was achieved using medium pressure 'Flash' column chromatography, with the use of Davisil silica 40–60 μm as the stationary phase, or Biotage automated chromatography using pre-packed silica cartridges. A Biotage SP4 automated flash purification system was used with UV monitoring at 298 nm and compound collection at 254 nm. Biotage KP-NH cartridges were employed for the separation of secondary, tertiary, and heterocyclic amines; using a primary amine (propyl amine) bonded silica. When stated, compounds were purified *via* semi-preparative HPLC, using an ACE 5 Phenyl 150 × 21.2 mm column using an Agilent 1200 Modular Preparative HPLC system.

Analytical techniques

All melting points were determined using a Stuart Scientific SMP3 or a Stuart Scientific SMP40 melting point apparatus and are uncorrected. ^{1}H and ^{13}C nuclear magnetic resonance (NMR) spectra were obtained as solutions in deuterated solvents DMSO-d_6, MeOD or $CDCl_3$ using a Bruker Avance III 500 spectrometer recording at 500 MHz. Chemical shifts (δ) are reported in parts per million (ppm) and the spin-multiplicity abbreviated as: s (singlet), d (doublet), t (triplet), q (quartet), quin (quintet), sept (septet), m (multiplet), or br (broad), with coupling constants (J) given in Hertz (Hz). Liquid chromatography – mass spectrometry (LC–MS) was carried out on a Micromass Platform LC running in both positive and negative electrospray mode with a PDA 240–400 nm detector using a Waters Symmetry Shield RP18 3 μm, 4.6 × 20 mm column with a flow rate of 3.0 mL min^{-1}. Alternatively, a Waters Acquity UPLC system was used, with a Waters SQD ESCi source using an Acquity UPLC BEH C18 1.7 μm, 2.1 × 50 mm column with a flow rate of 0.6 mL min^{-1}. The mobile phase used was 0.1 % v/v formic acid (aq.)/MeCN. Fourier transform infrared (FTIR) spectra were obtained using a Bio-Rad FTS 3000MX diamond ATR as a neat sample. Ultraviolet (UV) absorption data were collected using a Hitachi U-2800A spectrophotometer in ethanol. High-resolution mass spectra were performed by the ESPRC UK National Mass Spectrometry Facility, Swansea University, Singleton Park, Swansea, SA2 8PP. The purity of final compounds was assessed by reversed-phase HPLC; all tested compounds were >95% purity. HPLC instrument, Agilent 1200 equipped with a photodiode array detector (190–400 nm). Sample temperature, ambient; injection volume, 5 μL; flow rate, 1 mL min^{-1}. 5% to 100% MeCN gradient over 9 min and an isocratic hold at 100% MeCN for 2.5 min, before returning to initial conditions. Mobile phase A = 0.1% ammonia in water or 0.1% formic acid in water, mobile phase B = MeCN. Column: Waters XSELECT CSH C18, 3.5 μm, 4.6 mm × 150 mm or Waters XTerra RP18, 5 μm, 4.6 mm × 150 mm. Column maintained at ambient temperature.

Microwave assisted synthesis

When stated, reactions were carried out under microwave irradiation, in sealed vessels, using a Biotage Initiator Sixty with robotic sample bed. Samples were irradiated at 2.45 GHz, able to reach temperatures of 60–250 °C with a rate of heating at 2–5 °C s^{-1}, and pressures of up to 20 bar.

TBAF scavenger resin[32]

Amberlite 15 Ion exchange resin (SO_3H, 100 mL) was loaded into a column and washed with water (400 mL). The column was eluted with sat. calcium hydroxide solution whilst the pH of the eluent was monitored. Once the initially pH neutral eluent became strongly basic, the column was eluted with water until the pH of the eluent returned to neutral. The resin was washed with DCM (300 mL), THF (300 mL) and Et_2O (300 mL), before being removed from the column and dried in a vacuum oven at 40 °C.

General procedure A: TFA/TFE coupling of anilines with 2-fluoropurines using conventional heating

TFA (2.5–5.0 equiv.) was added to a solution of the purine substrate (1.0 equiv.) and the required aniline (2.0 equiv.) in TFE (10 mL mmol^{-1}). The reaction mixture was heated at reflux for 24 h unless otherwise stated, after which the solution was cooled and evaporated to dryness. The resulting residue was dissolved in EtOAc (10 mL mmol^{-1}) and washed with a saturated aqueous solution of $NaHCO_3$ (5 mL mmol^{-1}) and brine (5 mL mmol^{-1}). The combined aqueous layers were extracted with EtOAc (10 mL mmol^{-1}), and the combined organic extracts were dried ($MgSO_4$) and concentrated *in vacuo* to give the crude product for chromatographic purification.

General procedure B: removal of TIPS-protecting groups using TBAF

TBAF (1.2 equiv.) was added to a solution of the TIPS-protected substrate (1.0 equiv.) in THF (10–20 mL mmol^{-1}). The reaction mixture was stirred at RT for 5 min before being concentrated *in vacuo* and the crude residue purified by chromatography to afford the target compound.

6-Chloro-2-fluoro-9-(tetrahydro-2*H*-pyran-2-yl)-9*H*-purine (10)[33]

Part 1. To a stirred solution of HBF_4 (48% aqueous, 120 mL) at 0 °C, was added 2-amino-6-chloropurine (6.0 g, 35.0 mmol). Over 20 min, a solution of $NaNO_2$ (4.9 g, 70.0 mmol) in water (200 mL) was added dropwise, ensuring the temperature remained close to 0 °C. The pale yellow solution was raised to RT and stirred for 18 h. The resulting solution was neutralised to pH 7 in an ice bath at 0 °C by addition of Na_2CO_3 (6.00 g) in water (200 mL). The crude material was purified by chromatography on silica (10% MeOH/DCM) to afford 6-chloro-2-fluoropurine as a white crystalline solid (4.52 g, 75%); mp 171–173 °C (lit.,[34] mp 174 °C); λ_{max} (EtOH/nm) 393; IR (cm^{-1}) 2964, 2785, 1735, 1581; ^{1}H NMR (500 MHz, DMSO-d_6) 8.60 (1H, s, H-8), 13.9 (1H, s, NH-9); LRMS (ES^{+}) m/z 172.6 [M + H]$^{+}$.

Part 2. 3,4-Dihydropyran (60 μL, 0.58 mmol) was added dropwise over 10 min to a vigorously stirred solution of 6-chloro-2-fluoropurine (100 mg, 0.58 mmol) and (*rac*)-camphorsulfonic acid (5 mg, 0.02 mmol) in EtOAc (50 mL) at 65 °C. The temperature was maintained at 65 °C for 18 h. The resulting bright yellow solution was neutralised to pH 7 by careful addition of aqueous NH_3 solution, until a cloudy suspension persisted. The crude mixture was washed with brine (2 × 30 mL) and the aqueous phase was re-extracted with EtOAc (2 × 30 mL). The combined organic extracts were dried (Na_2SO_4) and purified by chromatography on silica (30% EtOAc/petrol). The desired compound was isolated as a pale yellow oil which solidified on refrigeration (110 mg, 75%); mp 69–70 °C (lit.[33] mp not available); λ_{max} (EtOH/nm)

269; IR (cm^{-1}) 3125, 2954, 2872, 2028, 1577; ^{1}H NMR (300 MHz, DMSO-d_6) 1.60 (2H, m, CH_2), 1.74 (1H, m, CH), 2.01 (2H, m, CH_2), 2.32 (1H, s, CH), 3.71 (1H, t, J = 12.0 Hz, CH), 4.01 (1H, d, J = 12.0 Hz, CH), 5.64 (1H, d, J = 12.0 Hz, CH), 8.25 (1H, s, H-8); LRMS (ES^+) m/z 257.7 $[M + H]^+$.

2-Fluoro-9-(tetrahydro-2*H*-pyran-2-yl)-6-((triisopropylsilyl)-ethynyl)-9*H*-purine (11). An oxygen-free solution of 6-chloro-2-fluoro-9-(tetrahydro-2*H*-pyran-2-yl)-9*H*-purine (**10**) (50 mg, 1.95 mmol), bis(triphenylphosphine)palladium(II) chloride (41 mg, 3.00 mol%) and copper iodide (7 mg, 2.00 mol%) in THF (10 mL) was degassed by bubbling nitrogen through the solution in a sealed Biotage microwave vial for 5 min. Triisopropylsilylacetylene (0.50 mL, 2.20 mmol) and triethylamine (0.70 mL, 4.90 mmol) were added to the mixture which was again degassed for 15 min. The solution quickly became dark red and stirring was continued at room temperature for 18 h. The black-brown suspension was filtered through Celite®, eluting with MeOH (3 × 20 mL). The product was purified by chromatography on silica (10% EtOAc/petrol) and isolated as a viscous yellow oil (78 mg, 99%); λ_{max} (EtOH/nm) 303.5; IR (cm^{-1}) 3433, 2945, 2865, 2705, 1702; ^{1}H NMR (500 MHz, DMSO-d_6) 1.15 (21H, m, $Si(CH(CH_3)_2)_3$ and $Si(CH(CH_3)_2)_3$), 1.60 (2H, m, CH_2), 1.75 (1H, m, CH), 1.99 (2H, m, CH_2), 2.19 (1H, s, CH), 3.74 (1H, t, J = 12.0 Hz, CH), 4.16 (1H, d, J = 12.0 Hz, CH), 5.69 (1H, d, J = 12.0 Hz, CH), 8.30 (1H, s, H-8); LRMS (ES^+) m/z 403.4 $[M + H]^+$.

2-Fluoro-6-(2-(triisopropylsilyl)ethynyl)-9*H*-purine (12). TFA (3 mL) was added to a solution of THP-protected purine **11** (0.644 g, 1.60 mmol) in IPA (15 mL). Water (3 mL) was added and the solution was heated to reflux for 2 h. The mixture was cooled and neutralised (conc. NH_3) before being extracted with EtOAc (3 × 50 mL) and the combined organic extracts dried ($MgSO_4$) and concentrated. The resulting residue was purified by chromatography on silica (30% EtOAc/petrol) to give the desired product as a pale yellow oil (0.461 g, 91%); R_f 0.25 (7 : 3 petrol/EtOAc); λ_{max} (EtOH/nm) 302; IR (cm^{-1}) 2945, 2866, 2361, 2000, 1584; ^{1}H NMR (500 MHz, DMSO-d_6) 1.12–1.21 (21H, m, $Si(CH(CH_3)_2)_3$), 8.68 (1H, s, H-8), 13.89 (1H, br, NH-9); HRMS calcd. for $C_{16}H_{24}FN_4Si$ (ES^+) m/z 319.1749 $[M + H]^+$, found 319.1752.

***N*-Phenyl-6-((triisopropylsilyl)ethynyl)-9*H*-purin-2-amine (13).** According to general procedure A, the title compound was prepared using: 2-fluoro-6-((triisopropylsilyl)ethynyl)-9*H*-purine (**12**) (0.70 g, 2.2 mmol) and aniline (0.40 mL, 4.4 mmol). The compound was isolated after chromatography (silica: 5% MeOH/DCM) followed by reversed phase column chromatography (C18 silica; 25% to 95% MeCN/water + 0.1% HCOOH), as a yellow oil (0.44 g, 47%); λ_{max} (EtOH/nm) 276; IR (cm^{-1}) 3389, 2361, 2021; ^{1}H NMR (500 MHz, $CDCl_3$) 1.13 (21H, m, $Si(CH(CH_3)_2)_3$), 7.02 (1H, t, J = 7.5 Hz, H-4′), 7.33 (2H, dd, J = 7.4, 7.5 Hz, H-3′ and H-5′), 7.80 (2H, d, J = 7.4 Hz, H-2′ and H-6′), 10.42 (1H, s, NH); LRMS (ES^+) m/z 392.0 $[M + H]^+$.

4-(6-((Triisopropylsilyl)ethynyl)-9*H*-purin-2-ylamino)-benzenesulfonamide (14). The title compound was synthesised following general procedure A using: 2-fluoro-6-((triisopropylsilyl)ethynyl)-9*H*-purine (**12**) (0.156 g, 0.49 mmol) and 4-aminobenzenesulfonamide (0.17 g, 0.98 mmol). The compound was purified using reversed phase column chromatography (C18 silica; 25% to 95% MeCN/water + 0.1% HCOOH), followed by trituration of the resulting oil using DCM, to obtain the product as a yellow solid (70 mg, 30%); m.p.163–165 °C; λ_{max} (EtOH/nm) 361.0, 291.0, 286.5, 215.5; IR (cm^{-1}) 3327, 2944, 2867, 1569, 1531, 1368, 1149; ^{1}H NMR (500 MHz, DMSO-d_6) 1.15 (21H, m, $Si(CH(CH_3)_2)_3$), 7.17 (2H, s, SO_2NH_2), 7.70 (2H, d, J = 9.0 Hz, H-2′ and H-6′), 7.95 (2H, d, J = 9.0 Hz, H-3′ and H-5′), 8.33 (1H, s, H-8); HRMS calcd. for $C_{22}H_{31}N_6O_2SSi$ $[M + H]^+$ 471.19874, found 471.19420.

6-Ethynyl-*N*-phenyl-9*H*-purin-2-amine (23). The TIPS-protected purine **13** (0.330 g, 0.84 mmol) and TBAF (1 M in THF, 930 μL, 0.93 mmol) were reacted in THF (10 mL) according to general procedure B, with purification by chromatography on silica (EtOAc) to give the desired product as a yellow solid (0.201 g, 100%); R_f 0.27 (EtOAc); mp 140–160 °C (decomposed); λ_{max} (EtOH/nm) 243; IR (cm^{-1}) 3414, 3111, 3072, 2920, 2110, 1704; ^{1}H NMR (500 MHz, DMSO-d_6) 4.86 (1H, s, C≡CH), 6.91–6.96 (1H, m, H-4′), 7.29 (2H, dd, J = 7.6 and 8.0 Hz, H-3′ and H-5′), 7.80 (2H, dd, J = 2.0 and 8.0 Hz, H-2′ and H-6′), 8.30 (1H, s, H-8), 9.70 (1H, s, NH), 13.17 (1H, br, NH-9); HRMS calcd. for $C_{13}H_{10}N_5$ (ES^+) m/z 236.0934 $[M + H]^+$, found 236.0931.

4-(6-Ethynyl-9*H*-purin-2-ylamino)benzenesulfonamide (24). Following general procedure B, the title compound was prepared using: TBAF solution (1.0 M in THF, 170 μL, 0.17 mmol) and 4-(6-((triisopropylsilyl)ethynyl)-9*H*-purin-2-ylamino)-benzenesulfonamide (**14**) (50 mg, 0.11 mmol) in THF (3 mL) to complete the deprotection after 5 min. The title compound was purified by chromatography on silica (10% MeOH/DCM) and isolated as a beige solid (18 mg, 50%); mp 156–158 °C; λ_{max} (EtOH/nm) 356.0, 292.5, 215.5; IR (cm^{-1}) 3347, 3255, 2920, 2848, 2118, 1568, 1529, 1477, 1128; ^{1}H NMR (500 MHz, DMSO-d_6) 4.90 (1H, s, C≡C–H), 7.16 (2H, s, SO_2NH_2), 7.17 (2H, d, J = 9.0 Hz, H-2′ and H-6′), 7.93 (2H, d, J = 9.0 Hz, H-3′ and H-5′), 8.36 (1H, s, H-8); HRMS calcd. for $C_{13}H_{11}N_6O_2S$ $[M + H]^+$ 315.0664, found 315.0687.

2-(3-(6-(2-(Triisopropylsilyl)ethynyl)-9*H*-purin-2-ylamino)-phenyl)acetic acid (59). 2-Fluoropurine intermediate **12** (1.06 g, 3.32 mmol) and 3-aminophenyl acetic acid (1.00 g, 6.64 mmol) were reacted with TFA (1.28 mL, 16.6 mmol) in TFE (25 mL) according to general procedure A. Upon completion of the reaction, the reaction solvent was removed *in vacuo* and the resultant residue was dissolved in THF (20 mL) and 1 M NaOH solution (15 mL). The mixture was stirred at RT for 18 h before the THF was removed *in vacuo*. The aqueous solution was then taken to pH 3 with 4 M HCl solution and extracted with EtOAc (3 × 75 mL). The combined organic extracts were dried (Na_2SO_4) and concentrated, and the resulting orange residue was purified by chromatography on silica (9 : 1 DCM/MeOH) followed by chromatography on reverse phase silica (9 : 1 MeOH/H_2O + 0.1% HCOOH). The desired product was obtained as an orange oil/gum (0.952 g,

64%); R_f 0.32 (9 : 1 DCM/MeOH); λ_{max} (EtOH/nm) 275; IR (cm^{-1}) 2972, 2360, 2340, 1977, 1702; ^1H NMR (500 MHz, DMSO-d_6) 1.13–1.22 (21H, m, Si(C*H*(CH_3)$_2$)$_3$), 3.51 (2H, s, CH_2CO_2H), 6.82–6.85 (1H, m, H-6′), 7.22 (1H, dd, J = 7.7 and 7.8 Hz, H-5′), 7.65–7.68 (1H, m, H-2′), 7.72–7.76 (1H, m, H-4′), 8.25 (1H, s, H-8), 9.71 (1H, s, NH), 12.33 (1H, br, CO_2H), 13.10 (1H, br, NH-9); HRMS calcd. for $C_{24}H_{32}N_5O_2Si$ (ES^+) m/z 450.2320 $[M + H]^+$, found 450.2320.

***N*-(4-Methoxybenzyl)-2-(3-(6-(2-(triisopropylsilyl)ethynyl)-9*H*-purin-2-ylamino)phenyl)acetamide (61).** CDI (0.140 g, 0.86 mmol) and DIPEA (150 μL, 0.86 mmol) were added to a solution of the carboxylic acid **59** (0.193 g, 0.43 mmol) in dry DMF (5 mL). The mixture was stirred at RT for 1.5 h, at which point 4-methoxybenzylamine (223 μL, 1.72 mmol) was added. Following a further 18 h stirring at RT, the solvent was removed *in vacuo* and the resulting residue was purified by chromatography on KP-NH silica (19 : 1 DCM/MeOH) gave the desired compound as a yellow oil/gum (0.238 g, 99%); R_f 0.48 (19 : 1 DCM/MeOH, KP-NH); λ_{max} (EtOH/nm) 277; IR (cm^{-1}) 2360, 2153, 2120, 1980; ^1H NMR (500 MHz, DMSO-d_6) 1.12–1.25 (21H, m, Si(C*H*(CH_3)$_2$)$_3$), 3.42 (2H, s, COCH_2), 3.71 (3H, s, OCH_3), 4.20 (2H, d, J = 5.8 Hz, NHCH_2), 6.85 (2H, d, J = 8.8 Hz, H-3″ and H-5″), 6.86–6.91 (1H, m, H-6′), 7.17 (2H, d, J = 8.8 Hz, H-2″ and H-6″), 7.20 (1H, dd, J = 7.9 and 8.0 Hz, H-5′), 7.59–7.62 (1H, m, H-2′), 7.74–7.78 (1H, m, H-4′), 8.24 (1H, s, H-8), 8.44 (1H, t, J = 5.8 Hz, N*H*CH_2), 9.65 (1H, s, NH), 12.06 (1H, br, NH-9); HRMS calcd. for $C_{32}H_{41}N_6O_2Si$ (ES^+) m/z 569.3055 $[M + H]^+$, found 569.3057.

2-(3-(6-(2-(Triisopropylsilyl)ethynyl)-9*H*-purin-2-ylamino)-phenyl)acetamide (63). PMB-amide **61** (0.232 g, 0.41 mmol) was dissolved in TFA (6 mL) and the resulting solution was heated at reflux for 72 h. The reaction mixture was evaporated to dryness and the resulting residue was dissolved in EtOAc (8 mL) and washed with a saturated aqueous solution of $NaHCO_3$ (2 × 4 m) and brine (4 mL). The combined aqueous layers were extracted with EtOAc (8 mL) and the combined organic extracts were dried ($MgSO_4$), concentrated *in vacuo* and the residue purified by chromatography on KP-NH silica (19 : 1 DCM/MeOH) gave the desired compound as a yellow oil/gum (0.170 g, 90%); R_f 0.24 (19 : 1 DCM/MeOH, KP-NH); λ_{max} (EtOH/nm) 276; IR (cm^{-1}) 3282, 2965, 2943, 2362, 1669; ^1H NMR (500 MHz, DMSO-d_6) 1.13–1.21 (21H, m, Si(C*H*(CH_3)$_2$)$_3$), 3.34 (2H, s, COCH_2), 6.83–6.86 (1H, m, H-6′), 6.88 (1H, s, CONH*H*′), 7.19 (1H, dd, J = 8.5 and 8.7 Hz, H-5′), 7.42 (1H, s, CONH*H*′), 7.57–7.60 (1H, m, H-2′), 7.72–7.76 (1H, m, H-4′), 8.23 (1H, s, H-8), 9.65 (1H, s, NH), 13.08 (1H, s, NH-9); HRMS calcd. for $C_{24}H_{33}N_6OSi$ (ES^+) m/z 449.2480 $[M + H]^+$, found 449.2480.

2-(3-(6-Ethynyl-9*H*-purin-2-ylamino)phenyl)acetamide (66). The TIPS-protected purine **63** (0.165 g, 0.37 mmol) was reacted with TBAF (1 M in THF, 0.55 mL, 0.55 mmol) in THF (4 mL) according to general procedure B. The residue was purified by semi-preparative HPLC (17 : 3 H_2O/MeCN), to give the desired compound as a yellow solid (0.084 g, 0.28 mmol, 76%); R_f 0.32 (17 : 3 DCM/MeOH, KP-NH); mp 250–270 °C (decomposed); λ_{max} (EtOH/nm) 274; IR (cm^{-1}) 3359, 3170, 2921, 2107, 1658; ^1H NMR (500 MHz, DMSO-d_6) 4.76 (1H, s, C≡CH), 6.77–6.81 (1H, m, H-6′), 6.83 (1H, s, CONH*H*′), 7.15 (1H, dd, J = 8.0 and 8.1 Hz, H-5′), 7.38 (1H, s, CONH*H*′), 7.47–7.50 (1H, m, H-2′), 7.68–7.73 (1H, m, H-4′), 8.19 (1H, s, H-8), 9.52 (1H, s, NH), 13.06 (1H, s, NH-9); HRMS calcd. for $C_{15}H_{13}N_6O$ (ES^+) m/z 293.1149 $[M + H]^+$, found 293.1145.

2,2,2-Trifluoroethyl(3-((6-((triisopropylsilyl)ethynyl)-9*H*-purin-2-yl)amino)phenyl)methanesulfonate (83). 2-Fluoropurine intermediate **12** (0.416 g, 1.31 mmol) and aniline **160** (0.704 g, 2.62 mmol) were reacted with TFA (504 μL, 6.54 mmol) in TFE (10 mL) according to general procedure A. The resulting orange oil was purified by chromatography on reverse phase silica (19 : 1 MeOH/H_2O + 0.1% HCOOH) followed by chromatography on silica (7 : 3 petrol/EtOAc) to give the desired compound as a yellow/orange oil/gum (0.506 g, 68%); R_f 0.34 (9 : 1 MeOH/H_2O, +0.1% HCOOH, C18); λ_{max} (EtOH/nm) 368, 277; IR (cm^{-1}) 2950, 2365, 2161, 2011, 1967, 1601; ^1H NMR (500 MHz, DMSO-d_6) 1.13–2.23 (21H, m, Si(C*H*(CH_3)$_2$)$_3$), 4.85 (2H, s, Ar–CH_2), 4.95 (2H, q, J = 8.7 Hz, F_3CCH_2O), 7.00–7.04 (1H, m, H-6′), 7.34 (1H, dd, J = 7.9 and 8.1 Hz, H-5′), 7.74–7.77 (1H, m, H-2′), 7.96–8.00 (1H, m, H-4′), 8.28 (1H, s, H-8), 9.84 (1H, s, NH), 13.12 (1H, br, NH-9); HRMS calcd. for $C_{25}H_{33}F_3N_5O_3SSi$ (ES^+) m/z 568.2020 $[M + H]^+$, found 568.2015.

***N*-(4-Methoxybenzyl)-1-(3-((6-((triisopropylsilyl)ethynyl)-9*H*-purin-2-yl)amino)phenyl)methanesulfonamide (84).** Trifluoroethyl sulfonate ester **83** (0.215 g, 0.38 mmol), 4-methoxybenzylamine (64 μl, 0.49 mmol) and DBU (115 μL, 0.76 mmol) were combined in dry THF (3 mL) in a sealed vial. The reaction mixture was heated under microwave irradiation at 160 °C for 15 min, before being evaporated to dryness. The resulting residue was dissolved in DCM (4 mL) and washed with a saturated aqueous solution of $NaHCO_3$ (4 mL), after which the biphasic mixture was passed through an Isolute® phase separator and the organic phase concentrated *in vacuo*. The crude residue was purified by chromatography on silica (19 : 1 DCM/MeOH) gave the desired compound as a yellow oil (0.224 g, 97%); R_f 0.44 (19 : 1 DCM/MeOH); λ_{max} (EtOH/nm) 276; IR (cm^{-1}) 2361, 2341, 2162, 1992, 1969, 1609; ^1H NMR (500 MHz, DMSO-d_6) 1.13–1.22 (21H, m, Si(C*H*(CH_3)$_2$)$_3$), 3.72 (3H, s, OCH_3), 4.05 (2H, d, J = 6.0 Hz, NHCH_2), 4.23 (2H, s, Ar–CH_2), 6.87 (2H, d, J = 8.7 Hz, H-3″ and H-5″), 6.91–6.95 (1H, m, H-6′), 7.23 (2H, d, J = 8.7 Hz, H-2″ and H-6″), 7.28 (1H, dd, J = 8.0 and 8.2 Hz, H-5′), 7.55 (1H, t, J = 6.0 Hz, N*H*CH_2), 7.72–7.75 (1H, m, H-2′), 7.87–7.91 (1H, m, H-4′), 8.26 (1H, s, H-8), 9.76 (1H, s, NH), 13.06 (1H, s, NH-9); HRMS calcd. for $C_{31}H_{41}N_6O_3SSi$ (ES^+) m/z 605.2725 $[M + H]^+$, found 605.2723.

(3-((6-((Triisopropylsilyl)ethynyl)-9*H*-purin-2-yl)amino)-phenyl)methanesulfonamide (85). PMB-sulfonamide **84** (0.221 g, 0.37 mmol) was dissolved in TFA (6 mL) and the resulting solution was heated at reflux for 3 h. The reaction mixture was evaporated to dryness and the resulting residue was dissolved in EtOAc (7 mL) and washed with a saturated aqueous solution of $NaHCO_3$ (2 × 4 mL) and brine (4 mL). The combined aqueous layers were extracted with EtOAc (7

mL) and the combined organic extracts were dried ($MgSO_4$), concentrated *in vacuo* and the residue purified by chromatography on KP-NH silica (19 : 1 DCM/MeOH) to give the desired compound as a yellow oil/gum (0.108 g, 60%); R_f 0.21 (19 : 1 DCM/MeOH, KP-NH); λ_{max} (EtOH/nm) 276; IR (cm^{-1}) 3367, 2943, 2865, 2160, 2021, 1606; ^1H NMR (500 MHz, DMSO-d_6) 1.13–1.23 (21H, m, Si(C*H*(CH_3)$_2$)$_3$), 4.21 (2H, s, Ar–CH_2), 6.84 (2H, s, SO_2NH_2), 6.95–6.98 (1H, br, H-6′), 7.13 (1H, dd, J = 7.9 and 8.0 Hz, H-5′), 7.68–7.71 (1H, m, H-2′), 7.90 (1H, ddd, J = 1.0, 1.9 and 8.0 Hz, H-4′), 8.25 (1H, s, H-8), 9.75 (1H, s, NH), 13.07 (1H, s, NH-9); HRMS calcd. for $C_{23}H_{33}N_6O_2SSi$ (ES^+) m/z 485.2149 $[M + H]^+$, found 485.2147.

(3-((6-Ethynyl-9*H*-purin-2-yl)amino)phenyl)-methanesulfonamide (87). TBAF (1 M in THF, 0.15 mL, 0.15 mmol) was added to a solution of TIPS-protected purine **85** (60 mg, 0.12 mmol) in THF (5 mL). The reaction mixture was stirred at RT for 5 min before being diluted with THF (12 mL) and the TBAF scavenger resin (0.60 g, 10× w/w) added. The resulting suspension was agitated at RT for 48 h, before being filtered and the filtrate concentrated *in vacuo*. The resulting residue was purified by chromatography on silica (9 : 1 DCM/MeOH) to afford the target compound as a pale yellow solid (23 mg, 58%); R_f 0.29 (9 : 1 DCM/MeOH); mp 190–210 °C (decomposed); λ_{max} (EtOH/nm) 273.5, 359.0; IR (cm^{-1}) 3361, 3248, 2976, 2809, 2707, 2114, 1701, 1610, 1583, 1491; ^1H NMR (500 MHz, DMSO-d_6) 4.22 (2H, s, SO_2CH_2), 4.85 (1H, s, C≡CH), 6.86 (2H, s, SO_2NH_2), 6.94–6.98 (1H, m, H-6′), 7.30 (1H, dd, J = 7.7 and 8.0 Hz, H-5′), 7.64–7.68 (1H, m, H-2′), 7.88–7.92 (1H, m, H-4′), 8.29 (1H, s, H-8), 9.72 (1H, s, NH), 13.13 (1H, br, NH-9); HRMS calcd. for $C_{14}H_{13}N_6O_2S$ (ES^+) m/z 329.0815 $[M + H]^+$, found 329.0821.

(*E*)-6-(2-(Azepan-1-yl)vinyl)-*N*-phenyl-9*H*-purin-2-amine (89)[14]. A solution of 6-ethynyl-*N*-phenyl-9*H*-purin-2-amine (**23**) (50 mg, 0.21 mmol) and homopiperidine (480 μL, 4.23 mmol) in anhydrous THF (2 mL) was subjected to microwave heating at 100 °C for 10 minutes in a sealed nitrogen flushed microwave vial (2–5 mL capacity). The cooled solution was partitioned between EtOAc (20 mL) and saturated $NaHCO_3$ solution (20 mL). The organic extract was concentrated *in vacuo* to a yellow/orange syrup which was subjected to purification by chromatography on KP-NH silica (9.5 : 0.5 DCM/MeOH), yielding the title compound as a yellow solid (69 mg, 98%); mp 135–137 °C (lit.,[14] mp 135–137 °C); λ_{max} (EtOH/nm) 360, 238, 254; IR (cm^{-1}) 3030, 2921, 2850, 1629, 1559; ^1H NMR (500 MHz, $CDCl_3$) 1.49 (4H, m, homopiperidine CH_2), 1.64–1.71 (4H, m, homopiperidine CH_2), 3.28–3.38 (4H, m, homopiperidine CH_2), 5.49–5.52 (1H, d, J = 15.0 Hz, C*H*═CH), 6.95–6.99 (1H, t, J = 10.5 Hz, H-4′), 7.19 (1H, s, H-8), 7.22–7.26 (2H, dd, J = 9.5, 10.5 Hz, H-3′ and H-5′), 7.32 (1H, br s, NH), 7.44–7.46 (2H, d, J = 9.5 Hz, H-2′ and H-6′), 8.23–8.26 (1H, d, J = 15.0 Hz, CH═C*H*), 12.89 (1H, br s, NH-9); HRMS calcd. for $C_{19}H_{22}N_6$ $[M + H]^+$ 335.1975, found 335.1979.

6-(2-(Azepan-1-yl)ethyl)-*N*-phenyl-9*H*-purin-2-amine (90). To a stirred solution of (*E*)-6-(2-(azepan-1-yl)vinyl)-*N*-phenyl-9*H*-purin-2-amine (**89**) (130 mg, 0.39 mmol) in THF (3 mL) was added sodium cyanoborohydride solution (1 M, in THF, 1.95 mL, 1.95 mmol) followed by TFA (3 μL, 0.04 mmol) or HCl (aq) (1 M, 40 μL, 0.04 mmol). Stirring was continued for 2 h (TFA) or 5 h (HCl), after which the solution was partitioned between EtOAc (20 mL) and saturated $NaHCO_3$ solution (10 mL). The organic extract was dried (Na_2SO_4) before purification by chromatography on KP-NH silica (9.5 : 0.5 DCM/MeOH) to yield a pale yellow solid (41 mg, 30%); mp 47–49 °C; λ_{max} (EtOH/nm) 326, 277, 238; IR (cm^{-1}) 2928, 2858, 1582; ^1H NMR (500 MHz, DMSO-d_6) 1.32–1.33 (4H, m, homopiperidine CH_2), 1.39–1.40 (4H, m, homopiperidine CH_2), 2.53–2.56 (4H, t, J = 5.5 Hz, homopiperidine NCH_2), 2.86–2.91 (2H, t, J = 8.0 Hz, CH_2), 2.92–2.98 (2H, t, J = 8.0 Hz, CH_2), 6.69–6.72 (1H, t, J = 8.5 Hz, H-4′), 7.05–7.08 (2H, dd, J = 7.5 and 8.5 Hz, H-3′ and H-5′), 7.65–7.66 (2H, d, J = 7.5 Hz, H-2′ and H-6′), 7.97 (1H, s, H-8), 9.21 (1H, br s, NH); HRMS calcd. for $C_{19}H_{25}N_6$ $[M + H]^+$ 337.2135, found 337.2138.

***N*-Phenyl-6-vinyl-9*H*-purin-2-amine (92).** *m*-CPBA (titrated as 62%, 30 mg, 0.108 mmol) was added in one portion to a stirred solution of 6-(2-(azepan-1-yl)ethyl)-*N*-phenyl-9*H*-purin-2-amine (**90**) (30 mg, 0.09 mmol) in anhydrous DCM (2 mL). The colourless solution instantly became bright yellow. After 2 h at room temperature the reaction was diluted with DCM (5 mL) and washed with saturated $NaHCO_3$ solution (4 mL). The crude product was purified by chromatography on silica (9.5 : 0.5 DCM/MeOH) to yield a yellow solid (6.4 mg, 30%); mp 121–123 °C; UV λ_{max} (EtOH) 270, 207; IR (cm^{-1}) 1578, 1532, 1496, 1439, 1392, 1349; ^1H NMR (500 MHz, DMSO-d_6) 5.84–5.86 (1H, dd, J = 1.5 and 12.5 Hz, *cis* CH═CH*H*), 6.86–6.89 (1H, dd, J = 1.5 and 17.5 Hz, *trans* CH═CH*H*), 7.01–7.04 (1H, t, J = 8.5 Hz, H-4′), 7.08–7.14 (1H, dd, J = 12.5 and 17.5 Hz, C*H*═CH_2), 7.24 (1H, s, H-8), 7.27–7.30 (2H, dd, J = 8.5 and 7.5 Hz, H-3′ and H-5′), 7.52–7.54 (2H, d, J = 7.5 Hz, H-2′ and H-6′); HRMS calcd. for $C_{13}H_{12}N_5$ $[M + H]^+$ 238.0509, found 238.0511.

6-Ethynyl-2-fluoro-9-(tetrahydro-2*H*-pyran-2-yl)-9*H*-purine (93)[17]. The TIPS-protected purine **11** (68 mg, 0.169 mmol) and TBAF (1 M in THF, 203 μL, 0.203 mmol) were reacted in THF (3 mL) according to general procedure B, with purification by chromatography on silica (15–100% EtOAc/petrol) to give the desired product as an off-white solid (41 mg, 100%); R_f 0.32 (50% EtOAc/petrol); ^1H NMR (500 MHz, $CDCl_3$) 1.58–1.63 (1H, m, C*H*), 1.63–1.78 (2H, m, CH_2), 1.90–1.99 (1H, m, C*H*), 1.99–2.06 (1H, m, C*H*), 2.07–2.12 (1H, m, C*H*), 3.68–3.74 (1H, m, C*H*), 3.71 (1H, s, C≡C*H*), 4.09–4.14 (1H, m, C*H*), 5.65 (1H, dd, J = 2.6 and 10.8 Hz, NC*H*), 8.26 (1H, s, H-8); LRMS (ES^+) m/z 247.0 $[M + H]^+$.

6-Ethyl-2-fluoro-9-(tetrahydro-2*H*-pyran-2-yl)-9*H*-purine (94). Lindlar's catalyst (10 mg, 20% w/w) was suspended in a stirred solution of **93** (50 mg, 0.20 mmol) and quinoline (20 μL, 0.16 mmol) in EtOAc (5 mL) under a balloon of H_2. After 2 h at room temperature the reduction was complete and the suspension was filtered through a plug of Celite, eluting with methanol (30 mL). Volatiles were removed *in vacuo* and the crude residue purified by chromatography on silica (50% EtOAc/petrol). The pure compound was isolated as a

colourless oil (50 mg, 99%); λ_{max} (EtOH/nm) 264; IR (cm^{-1}) 2946, 2860, 2364, 2338, 1604; ^{1}H NMR (500 MHz, DMSO-d_6) 1.35 (3H, t, J = 7.5 Hz, CH_3), 1.59 (2H, m, tetrahydropyran CH_2), 1.97 (1H, m, tetrahydropyran CH), 1.99 (2H, d, J = 10.5 Hz, tetrahydropyran CH_2), 2.50 (1H, m, tetrahydropyran CH), 3.01 (2H, q, J = 7.5 Hz, CH_2), 3.73 (1H, m, tetrahydropyran CH), 4.04 (1H, d, J = 10.5 Hz, tetrahydropyran CH), 5.69 (1H, d, J = 10.5 Hz, tetrahydropyran CH), 8.74 (1H, s, H-8); LRMS (ES^+) m/z 251.0 $[M + H]^+$.

6-Ethyl-2-fluoro-9*H*-purine (95). TFA (3 mL) was added to a solution of 6-ethyl-2-fluoro-9-(tetrahydro-2*H*-pyran-2-yl)-9*H*-purine (**94**) (0.18 g, 0.72 mmol) in IPA (15 mL). Water (3 mL) was added and the solution was heated to reflux for 2 h. The mixture was cooled and neutralised (conc. NH_3) before being extracted with EtOAc (3 × 50 mL) and the combined organic extracts dried ($MgSO_4$) and concentrated. The resulting residue was purified by chromatography on silica (25% EtOAc/petrol). The compound was isolated as a white solid (0.117 g, 98%); mp 146–148 °C; λ_{max} (EtOH/nm) 269; IR (cm^{-1}) 1676, 1616, 1573; ^{1}H NMR (400 MHz, DMSO-d_6) 1.30 (3H, t, J = 7.5 Hz, CH_3), 3.00 (2H, q, J = 7.5 Hz, CH_2), 8.17 (1 H, s, H-8); LRMS (ES^+) m/z = 167.7 $[M + H]^+$.

4-(6-Ethyl-9*H*-purin-2-ylamino)benzenesulfonamide (96). The title compound was synthesised according to general procedure A using: 6-ethyl-2-fluoro-9*H*-purine (**95**) (81 mg, 0.49 mmol) and 4-aminobenzenesulfonamide (0.17 g, 0.98 mmol). The compound was isolated after purification by chromatography on silica (50% EtOAc/petrol) as a white solid (33 mg, 21%); mp 291–293 °C; λ_{max} (EtOH/nm) 318, 287, 212; IR (cm^{-1}) 3377, 3060, 2852, 1388, 1158; ^{1}H NMR (500 MHz, DMSO-d_6) 1.35 (3H, t, J = 6.0 Hz, CH_3), 3.00 (2H, q, J = 6.0 Hz, CH_2), 7.14 (2H, br s, SO_2NH_2), 7.69 (2H, d, J = 7.5 Hz, H-2′ and H-6′), 7.99 (2H, d, J = 7.5 Hz, H-3′ and H-5′), 8.17 (1H, s, H-8), 9.89 (1H, br s, NH); HRMS calcd. for $C_{13}H_{15}N_6O_2S$ $[M + H]^+$ 319.0971, found 319.0979.

***N*^{2}-Phenylguanine 2,2,2-trifluoroacetate salt (98).** To a suspension of 2-bromohypoxanthine (1.00 g, 4.7 mmol) and aniline (0.9 mL, 9.40 mmol) in TFE (40 mL) was added TFA (1.80 mL, 23.5 mmol). The mixture was heated to reflux under nitrogen for 24 h. The mixture was filtered hot, washed with EtOH (3 × 50 mL g^{-1}), and air-dried for 30 min. The filtrate was evaporated *in vacuo* and the solid was recrystallised from EtOH to obtain the title compound as a white solid (1.17 g, 73%); mp 229–231 °C; λ_{max} (EtOH/nm) 272; IR (cm^{-1}) 3332, 3128, 2943, 2756, 2555, 2387, 1678, 1572; ^{1}H NMR (300 MHz, DMSO-d_6) 7.07 (1H, t, J = 7.5 Hz, H-4′), 7.36 (2H, dd, J = 7.5, 8.0 Hz, H-3′ and H-5′), 7.62 (2 H, d, J = 8.0 Hz, H-2′ and H-6′), 7.94 (1H, s, H-8), 8.46 (1H, br s, NH), 9.00 (1H, br s, NH); HRMS calcd. for $C_{11}H_{10}N_5O$ $[M + H]^+$ 228.0881, found 228.0880.

6-Chloro-*N*-phenyl-9*H*-purin-2-amine (99)[35]. *N*^{2}-Phenylguanine trifluoroacetate salt (**98**) (2.00 g, 5.87 mmol) and *N*,*N*-diethylaniline (1.9 mL, 11.73 mmol) was suspended in neat $POCl_3$ (30 mL) at room temperature. The reaction mixture was heated at 115 °C for 60 min under a nitrogen atmosphere. The resulting yellow solution was carefully added dropwise on to crushed ice in an ice bath with rapid stirring [CAUTION – VERY EXOTHERMIC]. Once addition was complete and the ice had melted, the homogeneous solution was neutralised to pH 7 by slow addition of NaOH solution (1.0 M), maintaining rapid stirring in an ice bath. The aqueous mixture was extracted with EtOAc (2 × 20 mL). The combined organic extracts were dried (Na_2SO_4) and purified by chromatography on silica (50% EtOAc/petrol). The title compound was isolated as a white solid (0.67 g, 46%); mp 172–174 °C (lit.[32] 155–160 °C); λ_{max} (EtOH/nm) 329, 272; IR (cm^{-1}) 3399, 3289, 1627, 1601, 1571, 1540; ^{1}H NMR (500 MHz, DMSO-d_6) 6.89–6.92 (1H, t, J = 7.5 Hz, H-4′), 7.23–7.26 (2H, dd, J = 7.4 and 7.5 Hz, H-3′ and H-5′), 7.71–7.73 (2H, d, J = 7.4 Hz, H-2′ and H-6′), 8.20 (1H, s, H-8), 9.81 (1H, br s, NH), 13.20 (1H, br s, NH-9); LRMS (ES^+) m/z 246.06 $[M + H]^+$.

6-Chloro-9-(4-methoxybenzyl)-*N*-phenyl-9*H*-purin-2-amine (100). 4-Methoxybenzylchloride (0.33 mL, 2.43 mmol) was added dropwise to a stirred solution of 6-chloro-*N*-phenyl-9*H*-purin-2-amine (**99**) (0.15 g, 0.6 mmol) and K_2CO_3 (0.25 g, 1.83 mmol) in anhydrous DMF (15 mL). The resulting solution was gently warmed to 60 °C under nitrogen for 18 h. Upon addition of water (50 mL) and brine (6 mL) to the mixture, a white precipitate was observed. The mixture was extracted with DCM (2 × 30 mL) and the combined organics dried (Na_2SO_4). The *N*-9 regioisomer was separated by column chromatography on silica (50% EtOAc/petrol) as a white crystalline solid (114 mg, 52%); mp 166–168 °C; λ_{max} (EtOH/nm) 274, 225; IR (cm^{-1}) 3286, 2834, 1599, 1511; ^{1}H NMR (500 MHz, DMSO-d_6) 3.74 (3H, s, OCH_3), 5.35 (2H, s, CH_2), 6.93–6.95 (2H, d, J = 9.0 Hz, H-3″ and H-5″), 6.98–7.01 (1H, t, J = 8.5 Hz, H-4′), 7.30–7.34 (2H, dd, J = 8.0 and 8.5 Hz, H-3′ and H-5′), 7.35–7.38 (2H, d, J = 9.0 Hz, H-2″ and H-6″), 7.76–7.79 (2H, d, J = 8.0 Hz, H-2′ and H-6′), 8.04 (1H, s, H-8), 9.80 (1H, br s, NH); LRMS (ES^+) m/z 365.1 $[M + 1]^+$.

6-Cyano-9-(4-methoxybenzyl)-2-(phenylamino)-9*H*-purine-6 (101). 6-Chloro-9-(4-methoxybenzyl)-*N*-phenyl-9*H*-purin-2-amine (**100**) (0.10 g, 0.27 mmol) was suspended in anhydrous MeCN (10 mL) and stirred at room temperature. Addition of tetraethylammonium cyanide (86 mg, 0.55 mmol) followed by DABCO (61 mg, 0.55 mmol) afforded a yellow homogenous solution which was stirred for a further 18 h under nitrogen. Excess cyanide was hydrolysed by addition of aqueous ammonium hydroxide solution (32% v/v, 30 mL) with stirring for an additional 1 h. The crude mixture was partitioned between DCM (20 mL) and brine (20 mL). The organic layer was isolated and dried (Na_2SO_4) before purification by column chromatography on silica (50% EtOAc/petrol). The required compound was obtained as a bright yellow solid (62 mg, 62%); mp 242–244 °C; λ_{max} (EtOH) 356, 276; IR (cm^{-1}) 4000, 3470, 3293, 3180, 2258, 1611, 1584, 1511, 1471, 1245; ^{1}H NMR (500 MHz, DMSO-d_6) 3.73 (3H, s, OCH_3), 5.36 (2H, s, CH_2), 6.93–6.95 (2H, dd, J = 8.0, 8.5 Hz, H-3′ and H-5′), 6.98–7.01 (1H, t, J = 8.5 Hz, H-4′), 7.34–7.39 (4H, m, H-2″, H-3″, H-5″ and H-6″), 7.73–7.75 (2H, d, J = 8.0 Hz, H-2′ and H-6′), 8.66 (1H, s, H-8), 10.11 (1H, br s, NH); LRMS (ES^+) m/z 357.2 $[M + H]^+$.

6-Cyano-2-(phenylamino)-9*H*-purine (102). 6-Cyano-9-(4-methoxybenzyl)-2-(phenylamino)-9*H*-purine (**101**) (50 mg, 0.14 mmol) was dissolved in TFA (2 mL). The deep orange solution was heated at 70 °C for 5 h. The reaction mixture was concentrated *in vacuo* and the resulting orange oil was redissolved in EtOAc (2 mL). Residual TFA was neutralised by washing the organic phase with aqueous $NaHCO_3$ (2 × 2 mL). The organic extract was dried (Na_2SO_4) and purified using reversed phase column chromatography on silica (70% MeOH/H_2O + 0.1% HCOOH) to obtain a bright yellow solid (13 mg, 40%); mp 247–249 °C (decomposed); λ_{max} (EtOH/nm) 387, 272; IR (cm^{-1}) 3389, 2255, 1601, 1537, 1496, 1396, 1348; ^{1}H NMR (500 MHz, DMSO-d_6) 7.01 (1H, t, J = 8.5 Hz, H-4′), 7.34 (2H, dd, J = 8.0 and 8.5 Hz, H-3′ and H-5′), 7.76 (2H, d, J = 8.0 Hz, H-2′ and H-6′), 8.52 (1H, s, H-8), 9.99 (1H, br s, NH), 13.60 (1H, br s, NH-9); HRMS calcd. for $C_{12}H_8N_6$ $[M+]^+$ 236.0738, found 236.0734.

Accession codes

X-ray co-crystal structures of Nek2 with compounds **24** (6SGD) and **66** (6SGH), and also with the competitively-binding control compounds **96** (6SGI) and **102** (6SGK) have been deposited with the PDB. Authors will release the atomic coordinates and experimental data upon article publication.

Ethical statement

All animal experiments performed were conducted under a UK Government Home Office License in accordance with relevant national laws. All procedures were reviewed and approved by the Newcastle University Animal Welfare Ethical Board and performed according to institutional guidelines.

Abbreviations used

CDI	1,1′-Carbonyldiimidazole
DIPEA	*N*,*N*-Diisopropylethylamine
HER2	Human epidermal growth factor receptor 2
MW	Microwave
NIMA	Never-in-mitosis gene A
PMB	4-Methoxybenzyl
S_NAr	Nucleophilic aromatic substitution
TFE	2,2,2-Trifluoroethanol

Author contributions

C. J. M. and C. R. C. contributed equally to the work described in this paper. C. J. M., synthesis and characterization of compounds; C. R. C., synthesis, characterization of compounds and manuscript preparation; R. B., project conception, experimental design and interpretation, data analysis and manuscript preparation; K. B., design, conduct and interpretation of Nek2 inhibition experiments; B. C., synthesis and characterization of compounds; A. M. F., project conception; I. R. H., project conception; S. J. H., data analysis and manuscript preparation; C. M-D., data collection and analysis of crystal structures; D. R. N., project conception, experimental design and interpretation and data analysis; M. W. R., crystal structure refinement, validation and data deposition; M. S., synthesis and characterization of compounds; D. T., synthesis and characterization of compounds; R. J. G., project conception, experimental design and interpretation and data analysis; B. T. G., experimental design and interpretation, data analysis and manuscript preparation; C. C., experimental design and interpretation, data analysis and manuscript preparation.

Conflicts of interest

There are no conflicts of interest to declare.

Acknowledgements

This research was supported by a grant from Cancer Research UK (Grant Reference C2115/A21421). RB acknowledges funding from Cancer Research UK (Grant References C24461/A10285, C24461/A23302). The use of the EPSRC Mass Spectrometry Service at the University of Wales (Swansea) is also gratefully acknowledged. Similarly, we thank beamline staff at The Diamond Light Source who provided excellent facilities for data collection.

References

1 S. R. Klutchko, H. Zhou, R. T. Winters, T. P. Tran, A. J. Bridges, I. W. Althaus, D. M. Amato, W. L. Elliott, P. A. Ellis, M. A. Meade, B. J. Roberts, D. W. Fry, A. J. Gonzales, P. J. Harvey, J. M. Nelson, V. Sherwood, H.-K. Han, G. Pace, J. B. Smaill, W. A. Denny and H. D. H. Showalter, Tyrosine kinase inhibitors. 19. 6-Alkynamides of 4-anilinoquinazolines and 4-anilinopyrido [3, 4-d] pyrimidines as irreversible inhibitors of the erbB family of tyrosine kinase receptors, *J. Med. Chem.*, 2006, **49**, 1475.

2 Q. Liu, Y. Sabnis, Z. Zhao, T. Zhang, S. J. Buhrlage, L. H. Jones and N. S. Gray, Developing irreversible inhibitors of the protein kinase cysteinome, *Chem. Biol.*, 2013, **20**, 46.

3 E. Anscombe, E. Meschini, R. Mora-Vidal, M. P. Martin, D. Staunton, M. Geitmann, U. H. Danielson, W. A. Stanley, L.-Z. Wang, T. Reuillon, B. T. Golding, C. Cano, D. R. Newell, M. E. M. Noble, S. R. Wedge, J. A. Endicott and R. J. Griffin, Identification and characterization of an irreversible inhibitor of CDK2, *Chem. Biol.*, 2015, **22**, 1159.

4 D. H. Wai, K. L. Schaefer, A. Schramm, E. Korsching, F. van Valen, T. Ozaki, W. Boecker, L. Schweigerer, B. Dockhorn-Dworniczak and C. Poremba, Expression analysis of pediatric solid tumor cell lines using oligonucleotide microarrays, *Int. J. Oncol.*, 2002, **20**, 441.

5 S. de Vos, W. K. Hofmann, T. M. Grogan, U. Krug, M. Schrage, T. P. Miller, J. G. Braun, W. Wachsman, H. P. Koeffler and J. W. Said, Gene expression profile of serial samples of transformed B-cell lymphomas, *Lab. Invest.*, 2003, **83**, 271.

6 D. G. Hayward, R. B. Clarke, A. J. Faragher, M. R. Pillai, I. M. Hagan and A. M. Fry, The centrosomal kinase Nek2 displays elevated levels of protein expression in human breast cancer, *Cancer Res.*, 2004, **64**, 7370.
7 Y. Fang and X. Zhang, Targeting NEK2 as a promising therapeutic approach for cancer treatment, *Cell Cycle*, 2016, **15**, 895.
8 https://depmap.sanger.ac.uk/.
9 M. Marina and H. I. Saavedra, Nek2 and Plk4: prognostic markers, drivers of breast tumorigenesis and drug resistance, *Front. Biosci.*, 2014, **19**, 352.
10 D. K. Whelligan, S. Solanki, D. Taylor, D. W. Thomson, K.-M. J. Cheung, K. Boxall, C. Mas-Droux, C. Barillari, S. Burns, C. G. Grummitt, I. Collins, R. L. M. van Montfort, G. W. Aherne, R. Bayliss and S. Hoelder, Aminopyrazine inhibitors binding to an unusual inactive conformation of the mitotic kinase Nek2: SAR and structural characterization, *J. Med. Chem.*, 2010, **53**, 7682.
11 S. Solanki, P. Innocenti, C. Mas-Droux, K. Boxall, C. Barillari, R. L. M. van Montfort, G. W. Aherne, R. Bayliss and S. Hoelder, Benzimidazole inhibitors induce a DFG-out conformation of never in mitosis gene A-related kinase 2 (Nek2) without binding to the back pocket and reveal a nonlinear structure–activity relationship, *J. Med. Chem.*, 2011, **54**, 1626.
12 P. Innocenti, K. M. J. Cheung, S. Solanki, C. Mas-Droux, F. Rowan, S. Yeoh, K. Boxall, M. Westlake, L. Pickard, T. Hardy, J. E. Baxter, G. W. Aherne, R. Bayliss, A. M. Fry and S. Hoelder, Design of potent and selective hybrid inhibitors of the mitotic kinase Nek2: Structure–activity relationship, structural biology, and cellular activity, *J. Med. Chem.*, 2012, **55**, 3228.
13 M. S. Cohen, C. Zhang, K. M. Shokat and J. Taunton, Structural bioinformatics-based design of selective, irreversible kinase inhibitors, *Science*, 2005, **308**, 1318.
14 C. R. Coxon, C. Wong, R. Bayliss, K. Boxall, K. H. Carr, A. M. Fry, I. R. Hardcastle, C. J. Matheson, D. R. Newell, M. Sivaprakasam, H. Thomas, D. Turner, S. Yeoh, L.-Z. Wang, R. J. Griffin, B. T. Golding and C. Cano, Structure-guided design of purine-based probes for selective Nek2 inhibition, *Oncotarget*, 2017, **8**, 19089.
15 H. Lebraud, C. R. Coxon, V. S. Archard, C. M. Bawn, B. Carbain, C. J. Matheson, D. M. Turner, C. Cano, R. J. Griffin, I. R. Hardcastle, U. Baisch, R. W. Harrington and B. T. Golding, Model system for irreversible inhibition of Nek2: thiol addition to ethynylpurines and related substituted heterocycles, *Org. Biomol. Chem.*, 2014, **12**, 141.
16 (*a*) A. Brathe, L.-L. Gundersen, J. Nissen-Meyer, F. Rise and B. Spilsberg, Cytotoxic activity of 6-alkynyl- and 6-alkenylpurines, *Bioorg. Med. Chem. Lett.*, 2003, **13**, 877; (*b*) F. Nagatsugi, K. Uemura, S. Nakashima, M. Maeda and S. Sasaki, 6-Vinylated guanosine as a novel cross-linking agent and its versatile synthesis from the 6-O-tosylate by Pd(0)-catalyzed cross-coupling, *Tetrahedron Lett.*, 1995, **36**, 421; (*c*) F. Nagatsugi, K. Uemura, S. Nakashima, M. Maeda and S. Sasaki, 2-Aminopurine derivatives with C6-substituted olefin as novel cross-linking agents and the synthesis of the corresponding β-phosphoramidite precursors, *Tetrahedron*, 1997, **53**, 3035; (*d*) M. Kuchar, R. Pohl, I. Votruba and M. Hocek, Synthesis of purines bearing functionalized C-substituents by the conjugate addition of nucleophiles to 6-vinylpurines and 6-ethynylpurines, *Eur. J. Org. Chem.*, 2006, 5083.
17 C. R. Coxon, E. Anscombe, S. J. Harnor, M. P. Martin, B. Carbain, B. T. Golding, I. R. Hardcastle, L. K. Harlow, S. Korolchuk, C. J. Matheson, D. R. Newell, M. E. M. Noble, M. Sivaprakasam, S. J. Tudhope, D. M. Turner, L.-Z. Wang, S. R. Wedge, C. Wong, R. J. Griffin, J. A. Endicott and C. Cano, Cyclin-dependent kinase (CDK) inhibitors: structure–activity relationships and insights into the CDK-2 selectivity of 6-substituted 2-arylaminopurines, *J. Med. Chem.*, 2017, **60**, 1746.
18 B. Carbain, C. R. Coxon, H. Lebraud, K. J. Elliott, C. J. Matheson, E. Meschini, A. R. Roberts, D. M. Turner, C. Wong, C. Cano, R. J. Griffin, I. R. Hardcastle and B. T. Golding, Trifluoroacetic acid in 2, 2, 2-trifluoroethanol facilitates SNAr reactions of heterocycles with arylamines, *Chem. – Eur. J.*, 2014, **20**, 2311.
19 H. D. Dakin and R. West, A general reaction of amino acids, *J. Biol. Chem.*, 1928, **78**, 91.
20 K.-V. Tran and D. Bickar, Dakin–West synthesis of β-Aryl Ketones, *J. Org. Chem.*, 2006, **71**, 6640.
21 C. Wong, R. J. Griffin, I. R. Hardcastle, J. S. Northen, L.-Z. Wang and B. T. Golding, Synthesis of sulfonamide-based kinase inhibitors from sulfonates by exploiting the abrogated SN 2 reactivity of 2, 2, 2-trifluoroethoxysulfonates, *Org. Biomol. Chem.*, 2010, **8**, 2457.
22 Y. Taniguchi, Y. Kurose, T. Nishioka, F. Nagatsugi and S. Sasaki, The alkyl-connected 2-amino-6-vinylpurine (AVP) crosslinking agent for improved selectivity to the cytosine base in RNA, *Bioorg. Med. Chem.*, 2010, **18**, 2894.
23 R. J. Griffin, A. Henderson, N. J. Curtin, A. Echalier, J. A. Endicott, I. R. Hardcastle, D. R. Newell, M. E. M. Noble, L.-Z. Wang and B. T. Golding, Searching for cyclin-dependent kinase inhibitors using a new variant of the cope elimination, *J. Am. Chem. Soc.*, 2006, **128**, 6012.
24 J. Ø. Madsen and P. E. Iversen, The stereochemical course of formic acid reduction of enamines, *Tetrahedron*, 1974, **30**, 3496.
25 J. Singh, R. C. Petter and A. F. Kluge, Targeted covalent drugs of the kinase family, *Curr. Opin. Chem. Biol.*, 2010, **14**, 475.
26 M. W. Richards, L. O'Regan, C. Mas-Droux, J. M. Y. Blot, J. Cheung, S. Hoelder, A. M. Fry and R. Bayliss, An autoinhibitory tyrosine motif in the cell-cycle-regulated Nek7 kinase is released through binding of Nek9, *Mol. Cell*, 2009, **36**, 560.
27 E. Leproult, S. Barluenga, D. Moras, J. M. Wurtz and N. Winssinger, Cysteine mapping in conformationally distinct kinase nucleotide binding sites: application to the design of selective covalent inhibitors, *J. Med. Chem.*, 2011, **54**, 1347.
28 J. Zhang, P. L. Yang and N. S. Gray, Targeting cancer with small molecule kinase inhibitors, *Nat. Rev. Cancer*, 2009, **9**, 28.

29 A. Chaikuad, P. Koch, S. A. Laufer and S. Knapp, The cysteinome of protein kinases as a target in drug development, *Angew. Chem., Int. Ed.*, 2018, 4372.
30 R. S. Hames, S. L. Wattam, H. Yamano, R. Bacchieri and A. M. Fry, APC/C-mediated destruction of the centrosomal kinase Nek2A occurs in early mitosis and depends upon a cyclin A-type D-box, *EMBO J.*, 2001, **20**, 7117.
31 J. Uetrecht, Idiosyncratic drug reactions: past, present, and future, *Chem. Res. Toxicol.*, 2007, **21**, 84.
32 J. J. Parlow, M. L. Vazque and D. L. Flynn, A mixed resin bed for the quenching and purification of tetrabutylammonium fluoride mediated desilylating reactions, *Bioorg. Med. Chem. Lett.*, 1998, **8**, 2391.
33 E. Winzeler, N. S. Gray, D. Han and D. Cheng, Compounds and compositions as kinase inhibitors, *WO2008094737A2*, 2008.
34 N. S. Gray, S. Kwon and P. G. Schultz, Combinatorial Synthesis of 2,9-Substituted Purines, *Tetrahedron Lett.*, 1997, **38**, 1161.
35 F. Focher, C. Hildebrand, S. Freese, G. Ciarrocchi, T. Noonan, S. Sangalli, N. Brown, S. Spadari and G. Wright, N2-Phenyldeoxyguanosine: A Novel Selective Inhibitor of Herpes Simplex Thymiding Kinase, *J. Med. Chem.*, 1988, **31**, 1496.